CRREL

REPORT 76-21

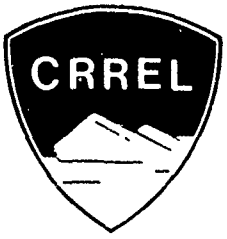

Compressibility characteristics of compacted snow

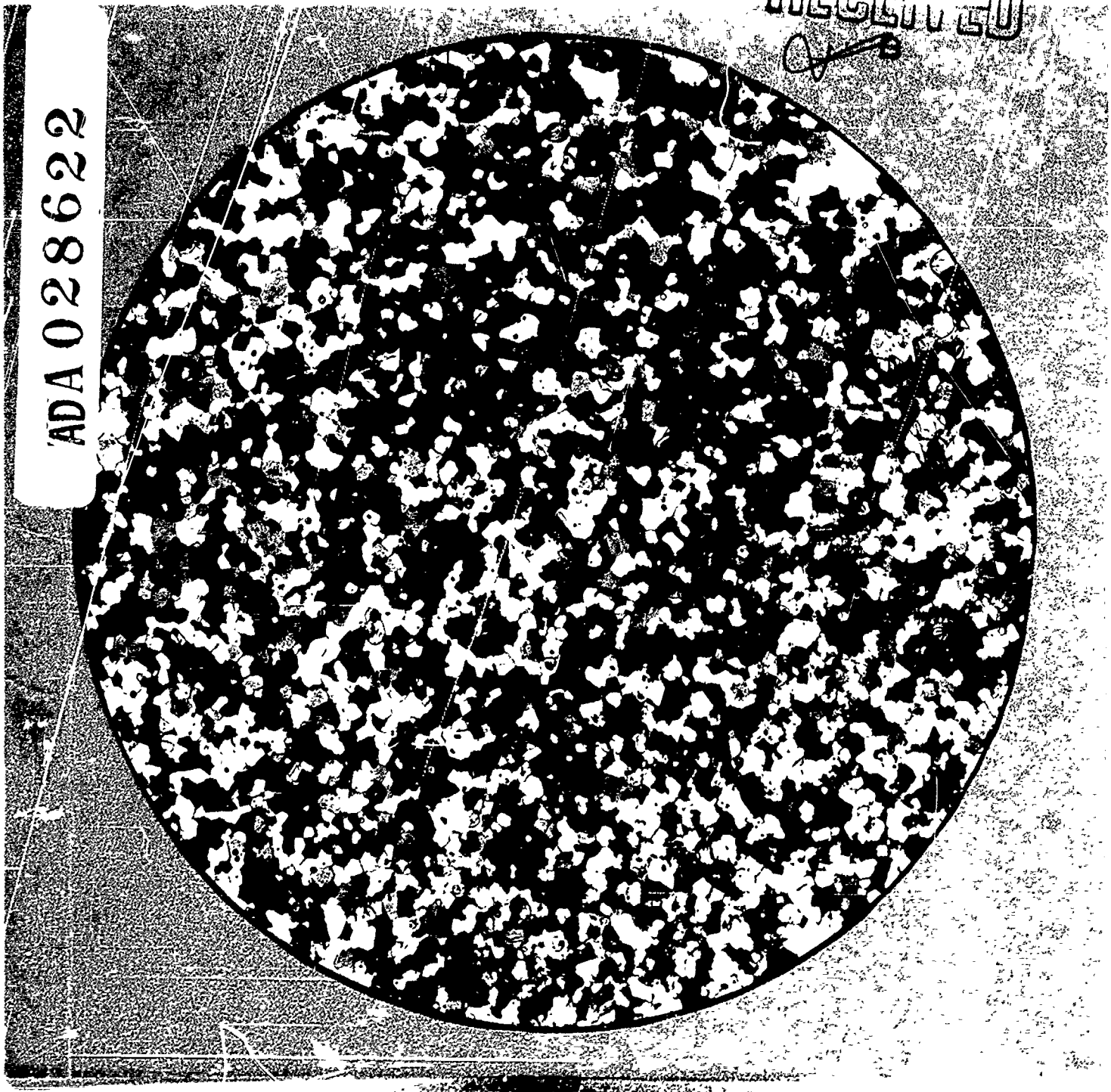

Cover: Thin section photograph of polycrystalline ice (magnified x 12) formed from snow compressed to 72 bars at -10°C. (Photograph by Anthony Gow.)

CRREL Report 76-21

Compressibility characteristics of compacted snow

Gunars Abele and Anthony J. Gow

June 1976

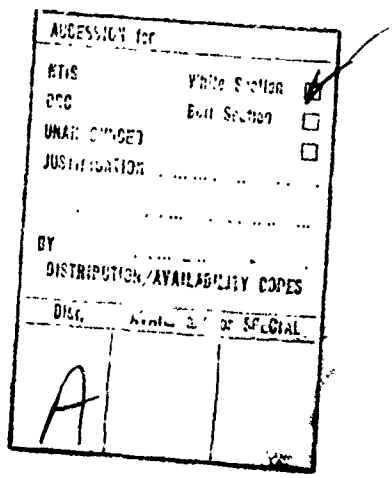

CORPS OF ENGINEERS, U.S. ARMY
COLD REGIONS RESEARCH AND ENGINEERING LABORATORY
HANOVER, NEW HAMPSHIRE

Factors for converting units of measurement to or from the SI metric system may be found in ASTM Standard E 380, Metric Practice Guide, *published by the American Society for Testing and Materials, 1916 Race St., Philadelphia, Pa. 19103.*

The findings in this report are not to be construed as an official Department of the Army position unless so designated by other authorized documents.

Unclassified

SECURITY CLASSIFICATION OF THIS PAGE *(When Data Entered)*

REPORT DOCUMENTATION PAGE

READ INSTRUCTIONS BEFORE COMPLETING FORM

1. REPORT NUMBER: CRREL ~~Report~~ 76-21	2. GOVT ACCESSION NO.
3. RECIPIENT'S CATALOG NUMBER	
4. TITLE *(and Subtitle)*: COMPRESSIBILITY CHARACTERISTICS OF COMPACTED SNOW	5. TYPE OF REPORT & PERIOD COVERED
	6. PERFORMING ORG. REPORT NUMBER
7. AUTHOR(s): Gunars Abele, Anthony J. Gow	8. CONTRACT OR GRANT NUMBER(s)
9. PERFORMING ORGANIZATION NAME AND ADDRESS: U.S. Army Cold Regions Research and Engineering Laboratory, Hanover, New Hampshire 03755	10. PROGRAM ELEMENT, PROJECT, TASK AREA & WORK UNIT NUMBERS: DA Project 4A161101A91D, Task 03, Work Unit 189
11. CONTROLLING OFFICE NAME AND ADDRESS: U.S. Army Cold Regions Research and Engineering Laboratory, Hanover, New Hampshire 03755	12. REPORT DATE: June 1976 13. NUMBER OF PAGES: 53
14. MONITORING AGENCY NAME & ADDRESS *(if different from Controlling Office)*: CRREL-76-21	15. SECURITY CLASS. *(of this report)*: Unclassified
	15a. DECLASSIFICATION/DOWNGRADING SCHEDULE

16. DISTRIBUTION STATEMENT *(of this Report)*

Approved for public release; distribution unlimited.

DA-H-A-161101891-D

17. DISTRIBUTION STATEMENT *(of the abstract entered in Block 20, if different from Report)*

18. SUPPLEMENTARY NOTES

cm/s.

19. KEY WORDS *(Continue on reverse side if necessary and identify by block number)*

Compressive properties	Snow
Crystals	Stresses
Mechanical properties	Trafficability

g/cu m.

20. ABSTRACT *(Continue on reverse side if necessary and identify by block number)*

The effects of snow temperature and initial density on the stress vs density and stress vs deformation relationships were investigated for shallow compacted snow in the density range of 0.28 to 0.76 g cm^{-3}, for a stress range of 0.5 to 72 bars and a temperature range of --1 to --34°C at a deformation rate of 40 $cm\ s^{-1}$. A decrease in temperature increases the resistance to stress, the effect increasing with applied stress. For any stress, an increase in the initial density results in an increase in the resulting density, the effect decreasing with an increase in stress. The approximate yield envelopes, which define the stress required to initiate any deformation of snow of a particular density and temperature, were determined. Rapid compaction of snow results in extensive recrystallization, significantly

(cont on p 1473 B)

20. Abstract (cont'd) for p 14 ; 3 #3

different from that of naturally compacted snow. At a stress of 72 bars, transformation to ice occurs only at temperatures above –10°C.

PREFACE

This study was conducted by Gunars Abele, Research Civil Engineer, Applied Research Branch, Experimental Engineering Division, U.S. Army Cold Regions Research and Engineering Laboratory; Dr. Anthony J. Gow, Research Geologist, Snow and Ice Branch, Research Division, CRREL, performed the microstructural analysis. The work was performed under DA Project 4A161101891D03, *In-House Laboratory Independent Research*, Work Unit 189.

Dr. Malcolm Mellor participated in the formulation of this study and technically reviewed the report. Larry Gould designed the sample containers. The Materials Testing System was operated by Allan George.

CONTENTS

ILLUSTRATIONS

Figure

TABLES

NOMENCLATURE

		Range
W	Load (kg)	Up to 9500
v	Rate of deformation (cm s^{-1})	40
T	Temperature (°C)	−1 to −34
ρ_0	Initial snow density (g cm^{-3})	0.28 to 0.76
ρ	Density at any time during load application (g cm^{-3})	
ρ_f	Final density (g cm^{-3})	up to 0.9
d	Sample diameter (cm)	12.7, 20.3, 29.0
h_0	Sample height (cm)	5.1, 7.6, 10.2
z	Vertical deformation of sample (cm)	up to 0.7 h_0
σ_1	Major principal stress (bar) (bar = 0.98 kg cm^{-2})	
σ_f	Final stress (bar)	up to 72
t	Age (after compaction)	2 hr to 7 days (Data from three 16-day old samples not used in analysis)

COMPRESSIBILITY CHARACTERISTICS OF COMPACTED SNOW

Gunars Abele and Anthony J. Gow

INTRODUCTION

The behavior of undisturbed, low density snow, when subjected to various rates of loading, has been studied previously and is discussed in an earlier report (Abele and Gow 1975). This study yielded some rather surprising results, specifically: the unexpectedly strong influence of the initial density on the stress-density relationship, the rather weak influence of snow temperature, and the weak influence of the deformation rate over the range studied.

The current study deals with the behavior of disturbed, higher density snow (compacted to various degrees) when subjected to uniaxial strain. That the compressibility characteristics of high density snow can not always be predicted by extrapolating data from low density snow will become evident from the new data shown in this report.

As in the previous study, the sample diameter to height ratio in these tests was from 2.5 to 5, thus representing the case of a finite snow layer on a rigid base.

DESCRIPTION OF STUDY

Sample preparation

Fifty-two snow samples were tested in circular sample containers. The following sizes of containers were used:

Inside diameter d (cm)	Height h_0 (cm)
12.7	2.5
12.7	5.1
20.3	5.1
20.3	7.6
29.0	10.2

The cylinders of the sample containers were removable from the baseplates to facilitate sample removal for final sample height measurements and preparation of thin sections for microstructural analysis. Both the baseplate and the inside wall of the cylinder were coated with Teflon. To

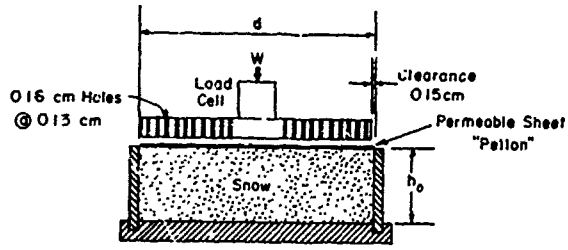

Figure 1. Test setup.

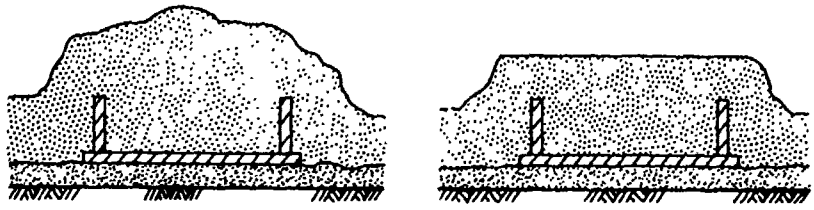

a. Collection of snow in sample container during snowfall.

b. Top of snow mound removed to produce a level surface.

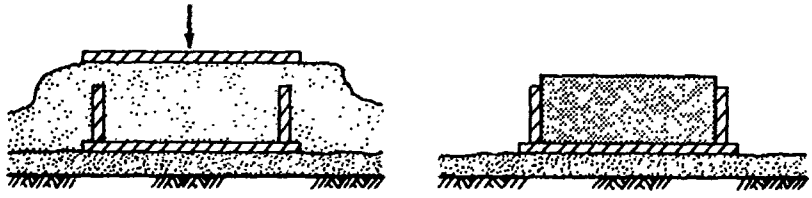

c. Compaction with a steel plate.

d. Snow sample before sealing in plastic bag and storage (sample will be shaved to be even with container top prior to test).

Figure 2. Sample preparation.

eliminate any friction between the load plate and the inside of the cylinder, a radial clearance of 0.15 cm was provided (Fig. 1). Small holes were drilled through the load plate to permit air escape from the sample during compression. A fitted sheet of Pellon, a material permeable to air but not to snow particles, was used between the surface of the snow sample and the load plate (Fig. 1).

Some samples were collected by placing the containers outside during various periods of snowfall. Excess snow was allowed to accumulate on top of the containers. Compaction was done by hand with a metal plate, as shown in Figure 2, to various degrees of density. The samples were then sealed in plastic bags and placed in coldrooms with temperatures of -1°, -10°, or -34°C for periods of 2 hours, 3 days, 7 days or 16 days (Table I). The temperature during the sample collection and compaction was between -1° and -7°C. The plastic bag was removed and the top surface of the snow shaved just before the sample was placed in the test chamber.

The exceptions to this sample preparation procedure were test samples 28-32. These samples were of snow which had been stored at -34°C for several weeks. The sample preparation and

Table I. Summary of tests.

Temp (°C)	Test sample no.	Identifying symbol of sample	Sample size: Diam d (cm)	Sample size: Height h_0 (cm)	Age (days)	Initial density ρ_0 (g cm^{-3})	Final density ρ_f (g cm^{-3})	Final stress σ_f (bar)
− 1	44	○	20.3	5.1	7	.30	.80	28
	42	□	12.7	5.1	7	.31	.91	72
	43	◇	12.7	5.1	7	.31	.91	72
	49	△	12.7	5.1	3	.46	.89	70
	50	▽	12.7	5.1	3	.47	.91	70
	52	◒	20.3	5.1	3	.49	.71	27
	51	◆	20.3	5.1	3	.52	.72	26
	41	▪	12.7	2.5	7	.58	.88	66
	1	■	12.7	5.1	0.1	.63	.89	68
	2	—	12.7	5.1	0.1	.66	.91	*
	5	▲	12.7	5.1	0.1	.66	.91	66
	3	—	12.7	5.1	0.1	.66	.91	*
	4	▼	12.7	5.1	0.1	.67	.91	66
− 4	32	◬	29.0	10.2	3	.36	.62	14
	28	—	29.0	10.2	3	.37	.63	*
	29	▨	29.0	9.0	3	.38	.62	14
	30	▨	29.0	9.6	3	.38	.61	14
	31	◈	29.0	9.9	3	.39	.62	14
−10	16	△	20.3	7.6	7	.28	.66	29
	13	▽	20.3	5.1	7	.29	.69	29
	14	□	20.3	5.1	7	.33	.68	29
	18	◬	20.3	7.6	7	.35	.67	28
	19	◬	12.7	5.1	7	.35	.80	72
	20	▽	12.7	5.1	7	.35	.80	72
	17	▽	20.3	7.6	7	.35	.66	29
	15	▨	20.3	5.1	7	.37	.69	28
	21	⊘	12.7	5.1	7	.40	.81	72
	11	◒	20.3	5.1	0.1	.50	.77	27
	12	◒	20.3	5.1	0.1	.50	.77	27
	6	◪	12.7	5.1	0.1	.51	.86	72
	10	◪	12.7	5.1	0.1	.51	.86	68
	9	◈	12.7	5.1	0.1	.52	.85	66
	7	◆	12.7	5.1	0.1	.52	.85	66
	8	◆	12.7	5.1	0.1	.53	.87	68
	33	●	20.3	7.6	7	.59	.75	28
	24	○	20.3	5.1	7	.30	.65	28
	34	—	20.3	5.1	7	.30	.65	*
	26	△	20.3	7.6	7	.30	.67	28
	37	—	12.7	5.1	16	.31	.75	72
	38	—	12.7	5.1	16	.32	.74	72
	25	□	20.3	5.1	7	.33	.65	28
	39	—	12.7	5.1	16	.34	.74	72
	22	◇	12.7	5.1	7	.34	.76	72
	27	◬	20.3	7.6	7	.35	.67	28
	23	▨	12.7	5.1	7	.36	.76	72
	47	▲	12.7	5.1	3	.45	.76	70
	46	▼	12.7	5.1	3	.45	.76	70
	48	◒	12.7	5.1	3	.48	.77	70
	45	◒	20.3	5.1	3	.50	.69	26
	35	◆	20.3	7.6	7	.53	.72	28
	36	■	20.3	7.6	7	.64	.71	28
	40	◆	12.7	2.5	7	.76	.79	68

* No oscilloscope trace for test samples 2, 3, 28, 34.

compaction were done at -4°C, and the samples were stored at that temperature for 3 days prior to testing.

Test equipment and procedure

The compression tests were conducted with a modern 10,000-kg load capacity servocontrolled MTS machine which is equipped with an environmental test chamber (temperature control to -50°C) and a closely calibrated ram speed control; the system is capable of any rate of deformation from 0 to 40 cm s^{-1}. The load vs ram displacement trace during a test is displayed and stored on the oscilloscope screen; a Polaroid photograph of the trace was taken after each test (see Appendix). The load and deformation data were obtained from the photographs.

After the snow sample was positioned in the test chamber, the load plate, which was attached to a load cell, was moved down to the top of the sample and the oscilloscope trace adjusted to the zero position. The MTS was set to the desired deformation rate, and the temperature in the chamber was checked.

All tests were performed to nearly the maximum load capability of the testing system. The maximum final stress σ_2 on the large diameter (29.0 cm) sample was, therefore, approximately 14 bars; for the medium diameter (20.3 cm) samples it was approximately 29 bars, and for the small diameter (12.7 cm) samples it was approximately 72 bars (1 bar = 0.98 kg cm^{-2}). The maximum rate of deformation, 40 cm s^{-1} (producing stain rates in the range of 1 to 10 s^{-1}) was used for all tests to simulate the rate of load application of a wheel or a track of a moving vehicle.

Immediately after the test, the sample was transferred to a coldroom (-10°C) where the sample was measured and weighed. The initial density was determined from the sample weight and the known initial volume; the final density was determined from measuring the height of the sample after the test. The density at any point during the test was computed with data from the load-deformation trace photograph.

Sections for the microscopic (thin section) inspection were taken from the samples after the volumetric measurements and stored at -35°C.

The test and sample conditions are listed in Table I. The range of the initial densities of the snow samples for each test temperature is shown graphically in Figure 3. This plot also serves to indicate the symbols which are later used in the stress-density graphs (Fig. 5 through 13) and the stress-deformation graphs (Fig. 20 through 26). The symbols are also shown in Table I next to the test sample numbers for convenient cross-referencing between the graphs and Table I.

Since the same rate of deformation was used for all tests, temperature was the only controlled, preselected parameter. Three test temperatures (dictated to some degree by the available coldrooms) were chosen: -1°, -10°, and -34°C. A few tests were performed at -4°C.

Snow density was not a closely controllable parameter. By varying the degree of compaction, a wide range of densities was obtained (from 0.28 to 0.76 g cm^{-3}). However, the density distribution was uneven, resulting in some gaps for each of the temperatures, such as in the 0.35 to 0.45 g cm^{-3} range for temperatures of -1° and -34°C and between 0.4 and 0.5 g cm^{-3} for the -10°C temperature (refer to Fig. 3).

The age of the snow samples (the time interval between sample preparation and test), although technically a controllable parameter, was not fully controllable in practice, since the use of the test equipment (the MTS was shared with other projects) could not always be scheduled for the same time interval after each snowfall. On a few occasions, equipment breakdown occurred when tests were scheduled. Consequently, an unplanned variable, the age of the sample, was introduced unintentionally. The age of each test sample is listed in Table I.

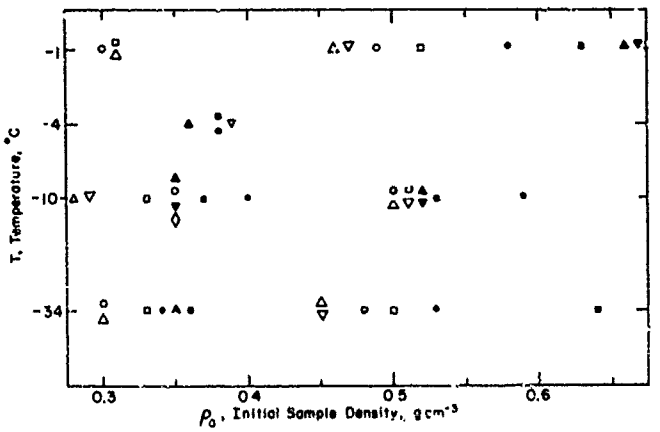

Figure 3. Range of sample densities (symbols are identified in Table I).

DISCUSSION OF RESULTS

Stress-density relationship

The range of the test data for both undisturbed snow (Abele and Gow 1975) and compacted snow from this study is shown in Figure 4.

The stress-density relationships are shown in the order of increasing initial density ρ_0 and decreasing temperature in Figures 5-13. The initial density of each test sample is shown in its relative position on the ρ scale at the bottom of each graph. The representative stress-density curves for a particular initial density were interpolated (or extrapolated) by eye from data on each graph.

The influence of the difference in sample age is noticeable in Figure 10. The curve for $\rho_0 = 0.5$ g cm^{-3} would lie somewhat higher (between the $\rho_0 = 0.6$ g cm^{-3} curve here and the $\rho_0 = 0.4$ g cm^{-3} curve in Fig. 9) if the age of the samples in the 0.50 to 0.53 g cm^{-3} density range were also somewhere around 7 days, instead of 2 hours. (Data from the three 16-day old samples, showing an even more noticeable difference, are not included in this set of graphs).

The stress-density curves for the various initial densities and temperatures in Figure 5 through 12 have been drawn as smooth lines. Closer inspection of the stress-density data for each test reveals that the snow samples with an initial density ρ_0 between 0.3 and 0.4 g cm^{-3} show, in most cases, a noticeable change in the curvature (a slight dip) of the stress-density relationship at a density ρ between 0.4 and 0.5 g cm^{-3}. Some of the more typical examples are shown in Figure 13. This phenomenon, which seems to appear at all test temperatures (refer to Fig. 8, 9, and 11), is masked to some degree when data from several tests are plotted on the same graph. Inspection of the previous data in the 0.1 to 0.2 g cm^{-3} initial density range (Abele and Gow 1975) does not reveal the presence of such a dip or curvature change. It is not clear why this phenomenon would be characteristic only of snow with an initial density between 0.3 and 0.4 g cm^{-3} when subjected to stress. Consequently, in Figures 14-16, which show the effect of initial density on the stress-density relationship at a particular temperature, the smooth curve method of representation was chosen.

It should also be noted that there may be another perceptible break in the stress-density relationship at a density of 0.65 g cm^{-3}. This becomes more evident if the stress-density relationship is treated as a straight line (on the semi-log plot) in the density range 0.45 to 0.65 g cm^{-3} (observe the data in Fig. 5, 6, 7, 9, 11, and 13).

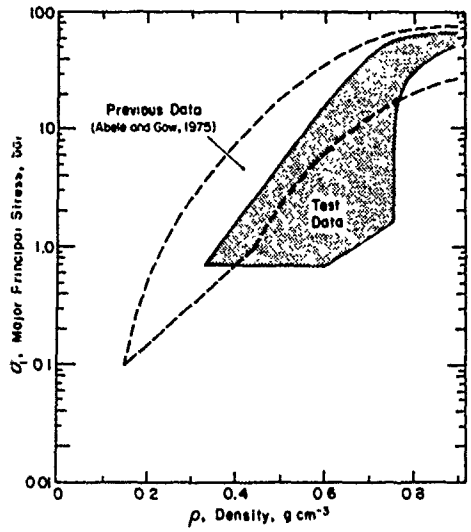

Figure 4. Range of test data.

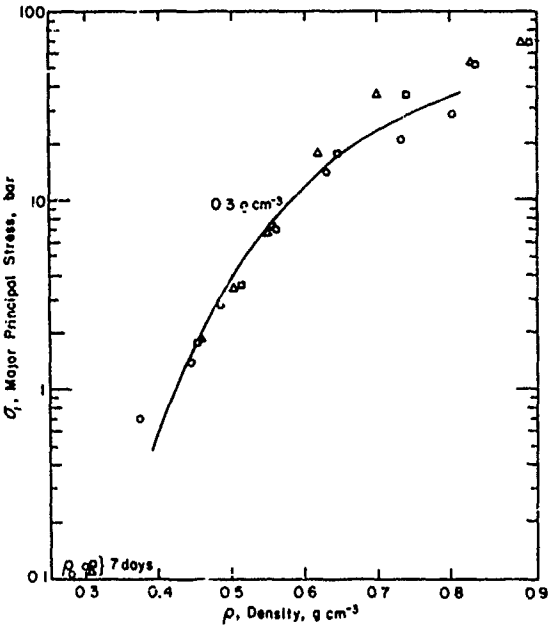

Figure 5. Major principal stress vs density at -1°C, initial density 0.30 to 0.31 g cm^{-3}.

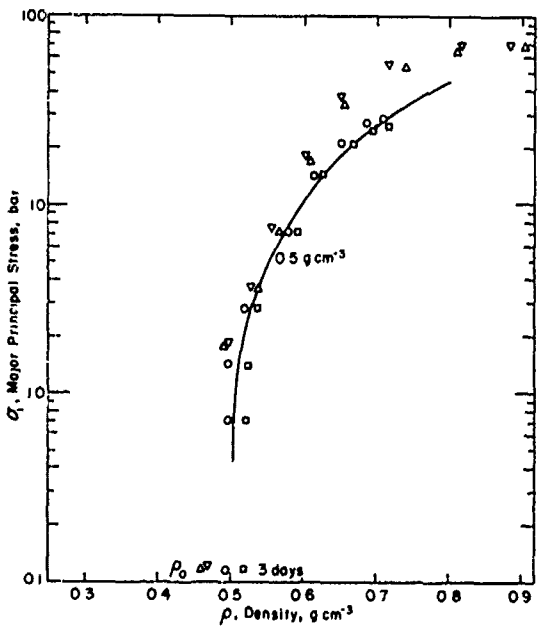

Figure 6. Major principal stress vs density at -1°C, initial density 0.46 to 0.52 g cm^{-3}.

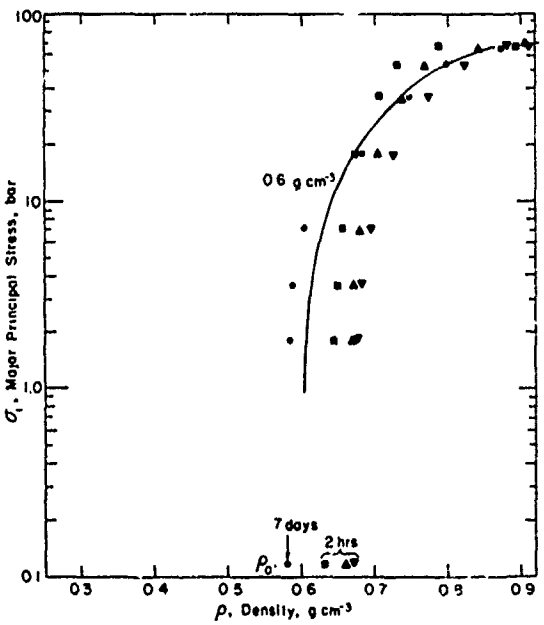

Figure 7. Major principal stress vs density at -1°C, initial density 0.58 to 0.67 g cm^{-3}.

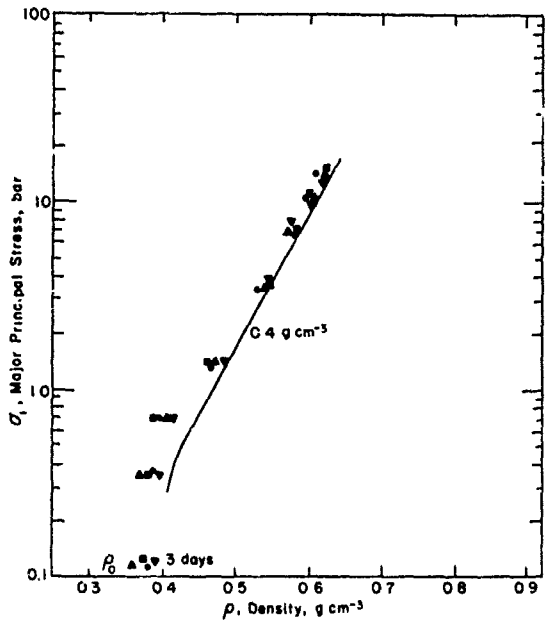

Figure 8. Major principal stress vs density at -4°C, initial density 0.36 to 0.39 g cm^{-3}.

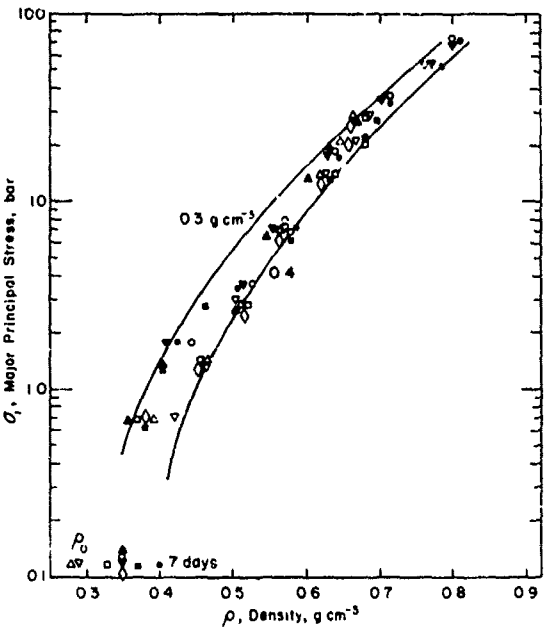

Figure 9. Major principal stress vs density at -10°C, initial density 0.28 to 0.40 g cm^{-3}.

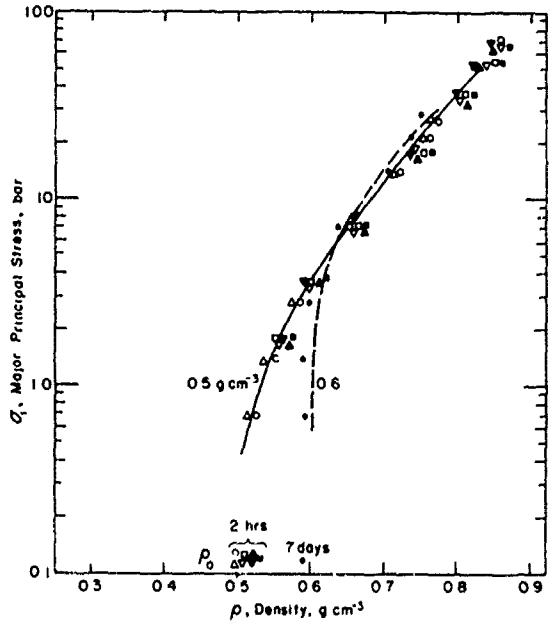

Figure 10. Major principal stress vs density at -10°C, initial density 0.50 to 0.59 g cm^{-3}.

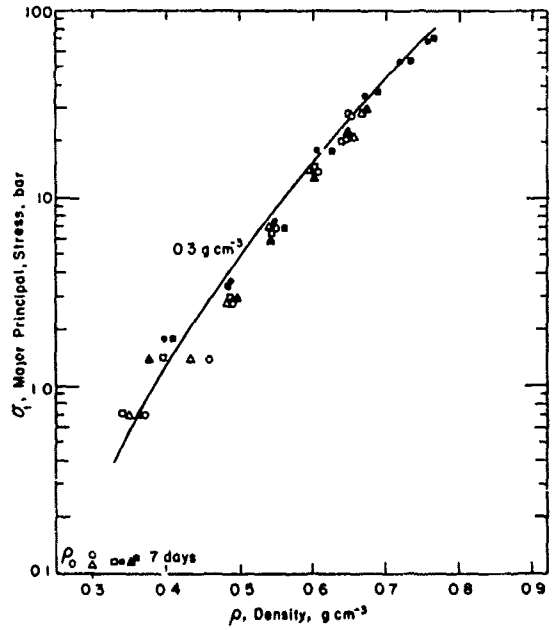

Figure 11. Major principal stress vs density at -34°C, initial density 0.30 to 0.36 g cm^{-3}.

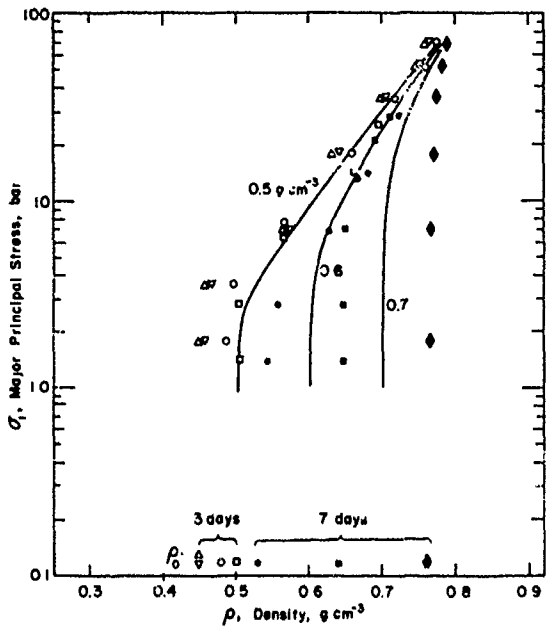

Figure 12. Major principal stress vs density at -34°C, initial density 0.45 to 0.76 g cm^{-3}.

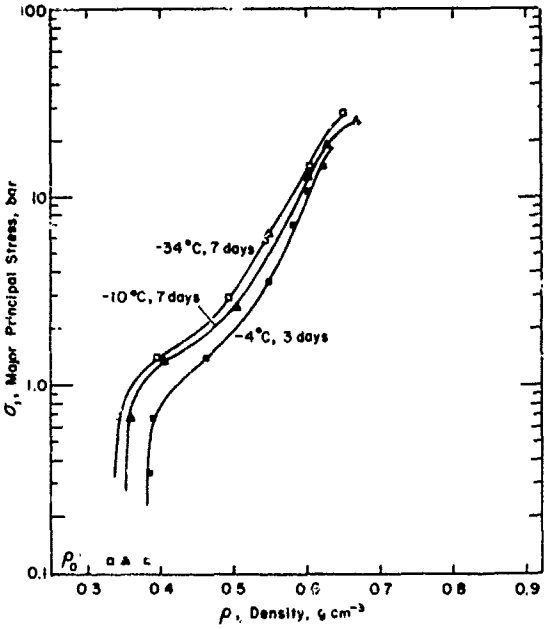

Figure 13. Some typical examples of the change in curvature in the stress-density relationship.

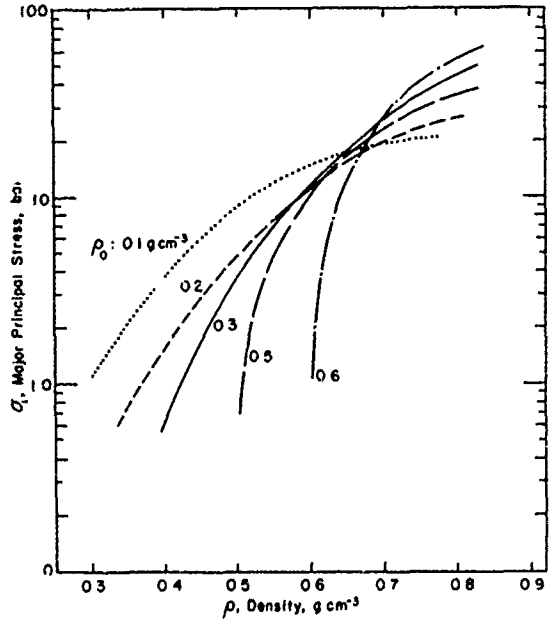

Figure 14. Summary of the stress-density relationships for various initial densities at -1°C. The 0.1 and 0.2 density curves are from Abele and Gow (1975).

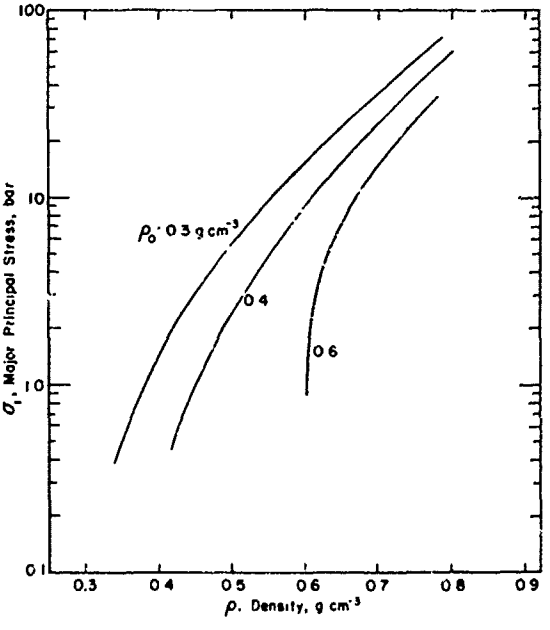

Figure 15. Summary of the stress-density relationships for various initial densities at -10°C.

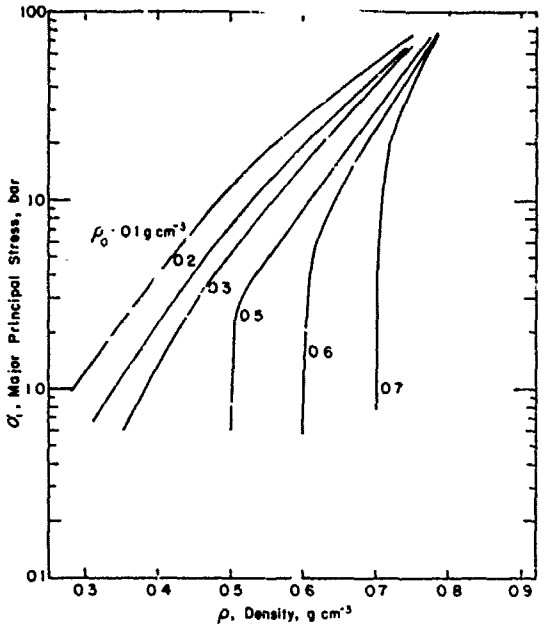

Figure 16. Summary of the stress-density relationships for various initial densities at -34°C. The 0.1 and 0.2 density curves are from Abele and Gow (1975).

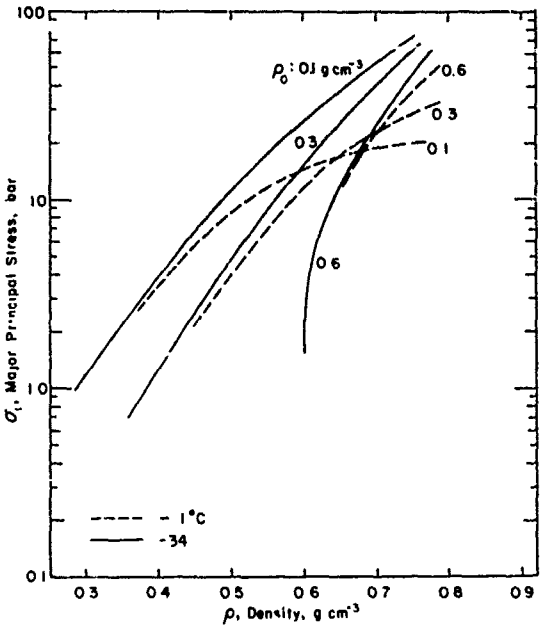

Figure 17. The effect of temperature on the stress-density relationship for various initial densities.

Figures 14-16 summarize the stress-density relationships of snow with various initial densities at temperatures -1°, -10° and -34°C, respectively. To achieve a density ρ of 0.6 g cm^{-3} or less at the relatively high temperature of -1°C (Fig. 14), the required stress varies inversely with the initial snow density (ρ_0). For example, to compact 0.1 g cm^{-3} density snow to a density of 0.5 g cm^{-3} requires a higher stress than that required to compact 0.3 g cm^{-3} density snow to a density of 0.5 g cm^{-3}. However, to reach densities above 0.7 g cm^{-3} at -1°C, the required stress increases with an increase in the initial density. This apparent change in behavior at a density of approximately 0.65 g cm^{-3}, when snows of various initial densities are subjected to stress at temperatures near 0°C, is a rather curious development. This behavior does not occur at -10° or -34°C (Fig. 15 and 16); here all the curves, representing the various initial snow densities, appear to converge toward a common point. In Figure 16, for example, an extrapolated stress of 100 bars on snow at -34°C will result in a density of approximately 0.8 g cm^{-3}, regardless of the initial snow density. At a temperature of -10°C, the same stress of 100 bars will compact snow to a density of 0.85 g cm^{-3} or more (Fig. 15).

The effects of temperature on the stress-density relationship for snows with initial densities of 0.1 (previous data), 0.3, and 0.6 g cm^{-3} are compared in Figure 17.

Figure 18 shows a summary of the stress-temperature relationships with density as a parameter for snow with initial densities of 0.3 and 0.5 g cm^{-3}. The data from only the 3- and 7-day old samples were used (the points in Figure 18 are from the curves shown in Figures 5, 6, 9, 11 and 12).

The effect of the initial snow density on the resulting density at a particular stress is shown in Figure 19. The new data for $\rho_0 > 0.3$ g cm^{-3} invalidate the assumption of Abele and Gow (1975) (an extrapolation made in the absence of any data) of how the ρ vs ρ_0 relationship approaches the upper boundary condition $\rho = \rho_0 = \rho_{ice}$ (refer to Fig. 8c and 8d in Abele and Gow 1975).

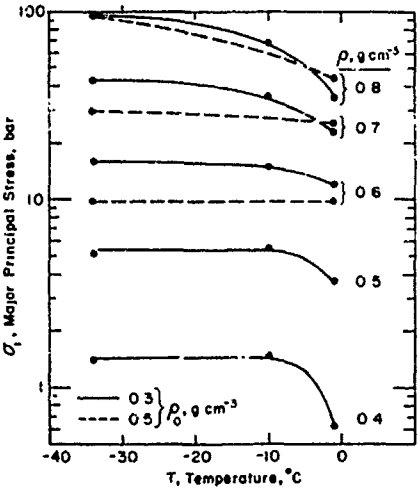

Figure 18. Major principal stress vs temperature with density as a parameter, initial density 0.3 and 0.5 g cm^{-3}.

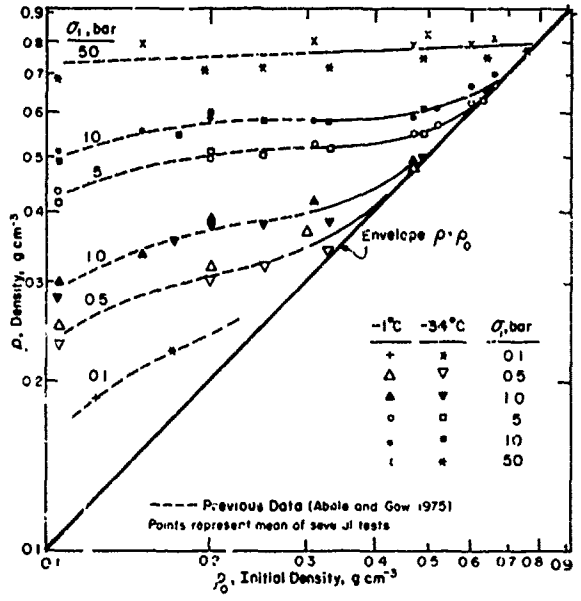

Figure 19. Density after load application vs initial density with stress as a parameter.

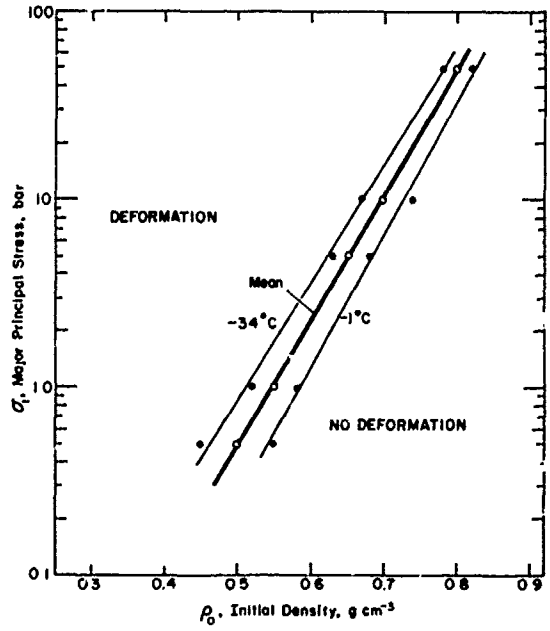

Figure 20. Yield envelopes for snow for a stress range between 0.5 and 50 bars.

The lines, in Figure 19, representing the ρ vs ρ_0 relationship at the various stress levels, intercept the $\rho = \rho_0$ envelope after a gradual, asymptotic-like approach. There is a point in the stress-density relationship which defines the stress required to initiate any deformation of snow of a particular density when load is applied at a rapid rate (40 cm s^{-1}). This is not applicable to a constant load condition or load application at a low rate. As load is applied at a constant rate of deformation, there is an instantaneous buildup in stress to a specific, critical point at which the resistance to stress of snow with particular characteristics (density, structure, age, temperature, etc.) is exceeded. Deformation then occurs, which may be gradual (e.g. Fig. 6 and 10), or display collapse behavior, as illustrated in Figure 13.

The scale of the oscilloscope traces used in these tests does not permit an accurate determination of this yield point. Consequently, the intercepts of the ρ vs ρ_0 curves with the $\rho = \rho_0$ envelope in Figure 19, which define the density at which deformation begins to occur for a particular stress, were estimated by eye and are plotted at the mean value between -1°C and -34°C in Figure 20. The estimated intercept values for the ρ vs ρ_0 data at the -1° and -34°C temperatures are also shown individually in Figure 20, but these estimated values are even less reliable than the mean values. The

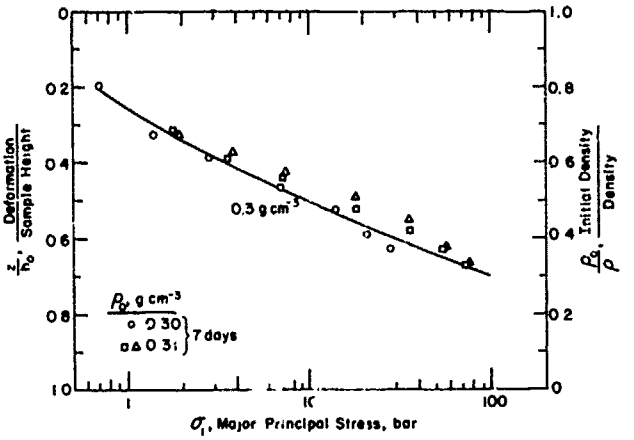

Figure 21. Consolidation vs major principal stress at -1°C, initial density 0.30 to 0.31 g cm^{-3}.

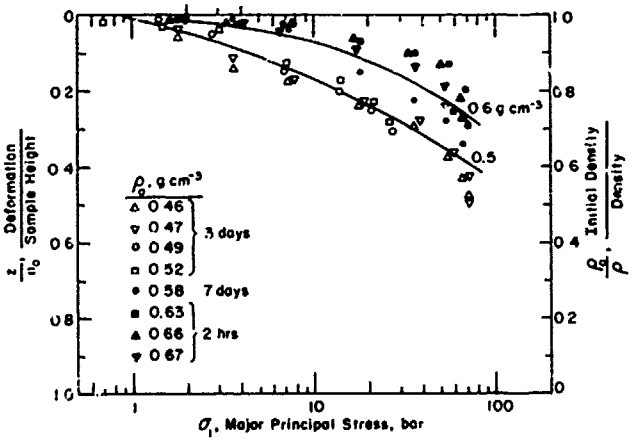

Figure 22. Consolidation vs major principal stress at -1°C, initial density 0.46 to 0.67 g cm^{-3}.

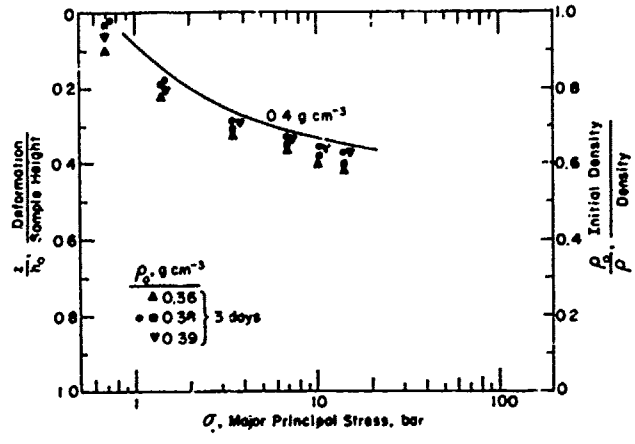

Figure 23. Consolidation vs major principal stress at -4°C, initial density 0.36 to 0.39 g cm^{-3}.

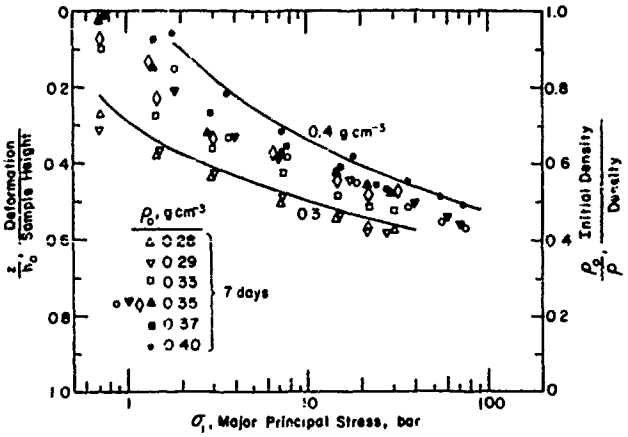

Figure 24. Consolidation vs major principal stress at -10°C, initial density 0.28 to 0.40 g cm^{-3}.

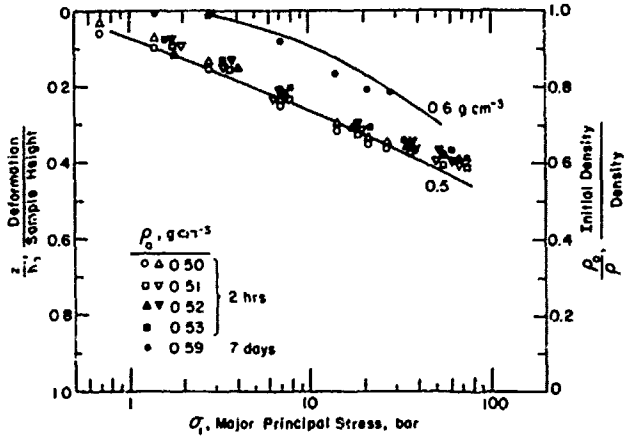

Figure 25. Consolidation vs major principal stress at -10°C, initial density 0.50 to 0.59 g cm^{-3}.

lines in Figure 20 represent the envelopes which define the approximate yield point of snow of a particular density (between 0.5 and 0.8 g cm^{-3}) in the temperature range of -1° to -34°C.

For example, to cause any deformation in compacted snow of several days age to a density of 0.5 g cm^{-3} would require a stress of approximately 0.5 bar at a temperature of about -16°C (mean curve in Fig. 20); for a 0.8 g cm^{-3} density the required stress would be 50 bars.

Stress-deformation relationship

The stress-deformation (pressure-sinkage) behavior of snow, which is of a more practical significance for snow trafficability analyses than the stress-density relationship, is shown in Figures 21-27 for the various initial densities and temperatures. Since the initial plotting of stress vs vertical deformation (sinkage) z for the various sample heights h_0 in the 5.1 to 10.2 cm range did not show any noticeable influence of the sample height, it was possible to collapse the data into a nondimensional deformation/sample height (i.e. engineering strain) form, which is also the inverse of the ratio of initial density to resulting density. The curves in Figures 21-27 for a particular initial density were interpolated (or extrapolated) from the data on each graph.

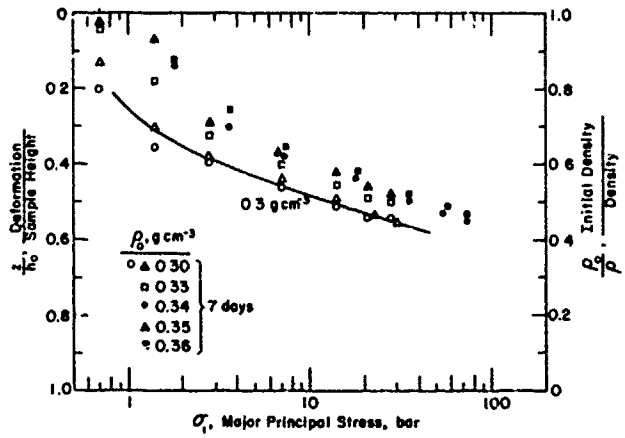

Figure 26. Consolidation vs major principal stress at -34°C, initial density 0.30 to 0.36 g cm^{-3}.

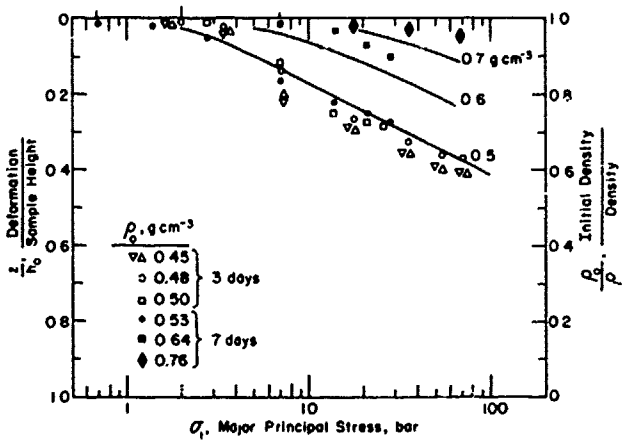

Figure 27. Consolidation vs major principal stress at -34°C, initial density 0.45 to 0.76 g cm^{-3}.

The effect of temperature on the stress-deformation relationship is shown in Figures 28-31 by plotting consolidation (z/h_0) vs temperature with initial density as a parameter for various stress levels (1, 5, 10 and 50 bars). The data for the 0.50 to 0.53 g cm^{-3} density range at -10°C are also shown, although the data do not fit very well because of the low age of 2 hours. The interpolated lines for the z/h_0 vs T relationship, as a function of ρ_0, show the lack of any significant temperature effect. (Plotting stress vs the ratio of ρ_0/ρ as in Figures 21-27, instead of stress vs ρ, results in minimizing the evidence of the temperature effect).

The stress-deformation (consolidation) relationships for the various initial densities for the -1° to -34°C temperature range are summarized in Figure 32. The curves for 0.1 and 0.2 g cm^{-3} initial density are from previous data (Abele and Gow 1975).

Consolidation as a function of initial density, with stress as a parameter, is plotted in Figure 33. The dashed lines, for $\rho_0 < 0.2$ g cm^{-3}, are again from the previous data. The intercepts on the ρ_0 axis (density at which no deformation occurs at a particular stress), which have to be estimated by eye as in Figure 19, correspond to the points on the mean envelope in Figure 20.

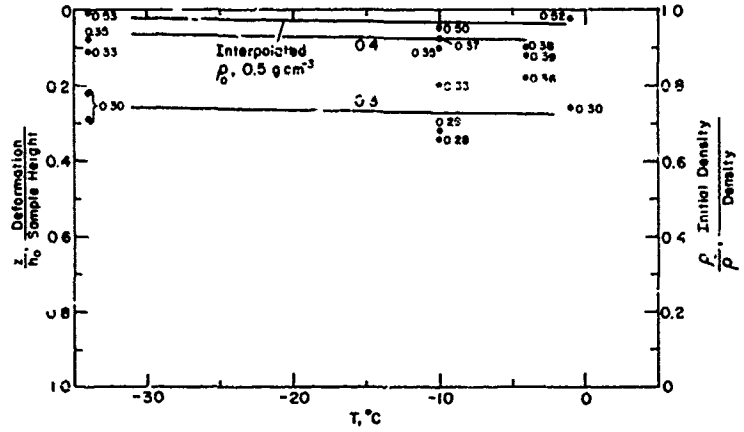

Figure 28. Consolidation vs temperature with initial density as a parameter for stress of 1 bar.

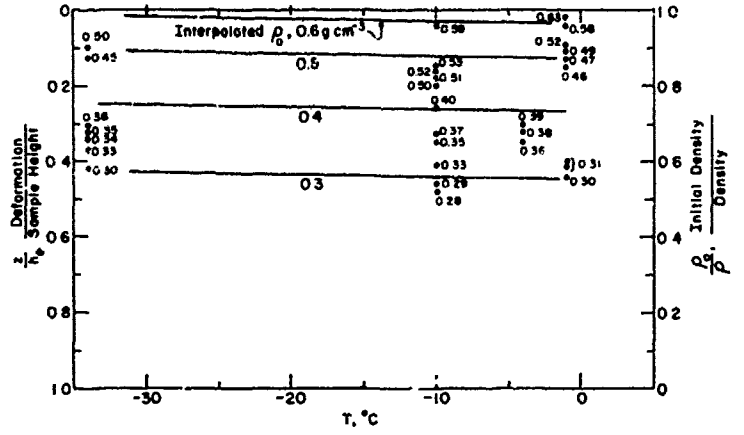

Figure 29. Consolidation vs temperature with initial density as a parameter for stress of 5 bars.

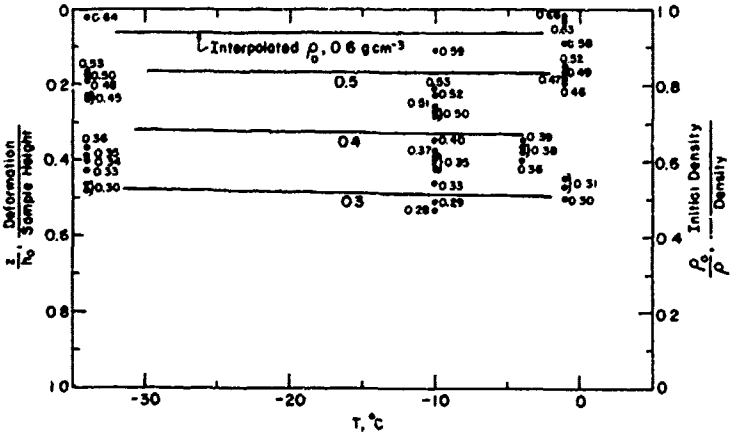

Figure 30. Consolidation vs temperature with initial density as a parameter for stress of 10 bars.

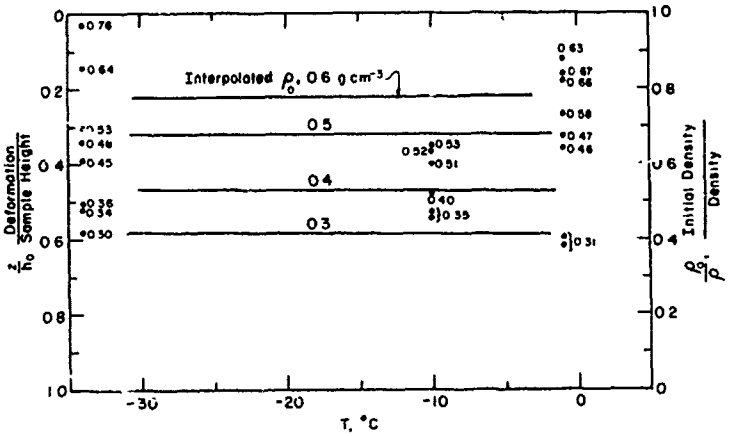

Figure 31. Consolidation vs temperature with initial density as a parameter for stress of 50 bars.

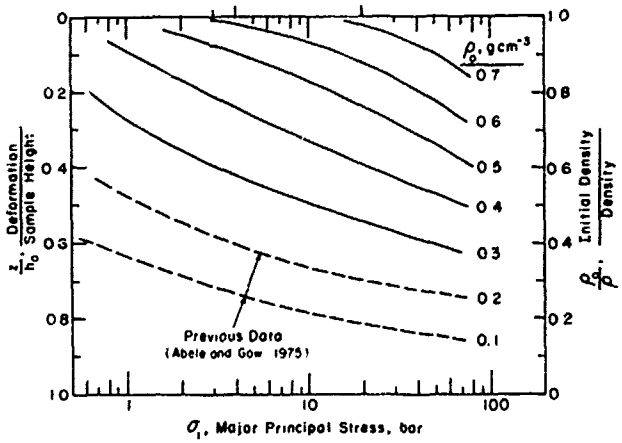

Figure 32. Summary of the stress-consolidation relationships for various initial densities.

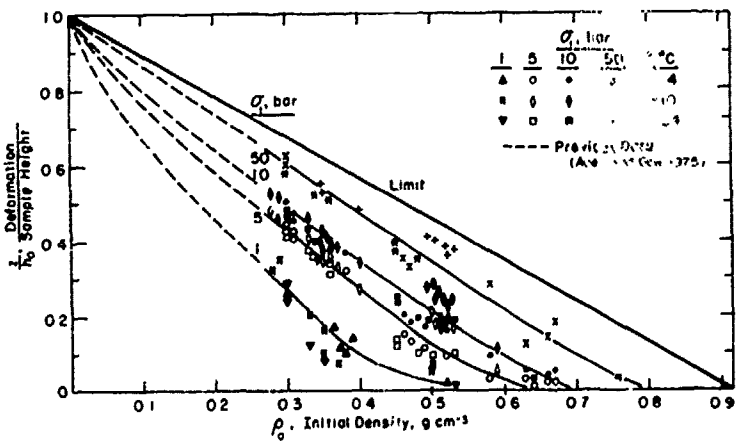

Figure 33. Consolidation vs initial density with stress as a parameter.

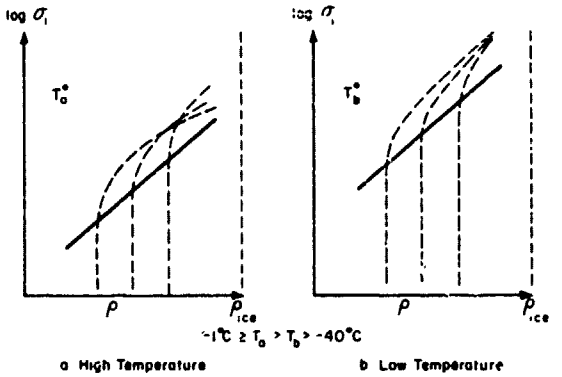

Figure 34. The general behavior of snow under increasing stress as a function of initial density and temperature.

SUMMARY AND CONCLUSIONS

Laboratory tests, using a modern 10,000-kg capacity MTS machine equipped with an oscilloscope with load-deformation trace storage, were conducted on shallow, compacted snow samples on a rigid base under uniaxial load to determine the stress vs density and stress vs deformation relationships as influenced by temperature (-1° to -34°C) and initial density (0.28 to 0.76 g cm^{-3}) in the pressure range of 0.5 to 72 bars at a deformation rate of 40 cm s^{-1} (producing strain rates in the range of 1 to 10 s^{-1}).

A decrease in temperature increases the resistance to stress and deformation, the temperature effect increasing with applied pressure and snow density. At stress levels below 10 bars, the temperature effect is evident only at temperatures near 0°C. The effect of temperature during load application at a high rate is not evident or has very little influence in the temperature range of -10° to -34°C at stresses below 10 bars.

Previous work (Abele and Gow 1975) showed the effect of the initial density of undisturbed snow at low stress levels (< 10 bars) at temperatures near 0°C, the resulting density at any stress increasing with initial density. This effect becomes less evident for higher initial densities and higher stress levels.

The general behavior of snow under increasing stress as a function of initial density and temperature is illustrated in Figure 34.

The estimated yield envelopes, which define the stress required to initiate deformation of snow of a particular density during rapid load application, are shown in Figure 35 superimposed on Mellor's (1974) Figure 13 (also Figure 2 in Abele and Gow 1975). The envelopes appear to agree when extrapolated with region A (natural densification), the lower limit for the family of compressibility curves.

In a stress-deformation (or pressure-sinkage) plot, the behavior of a shallow, confined snow sample on a rigid base corresponds to the compaction case (Assur 1964) for all densities (σ_1 plotted on arithmetic scale), as would be expected in the case of a high load size vs snow depth ratio $d/h_0 \geq 5$. In the case of a load on deep snow, where the d/h_0 ratio is very small, the snow behavior corresponds to the fluidization case for snow densities below 0.45 g cm^{-3} at low z/h_0 ratios (Abele 1970). A comparison of the two test condition cases is shown in Figure 36.

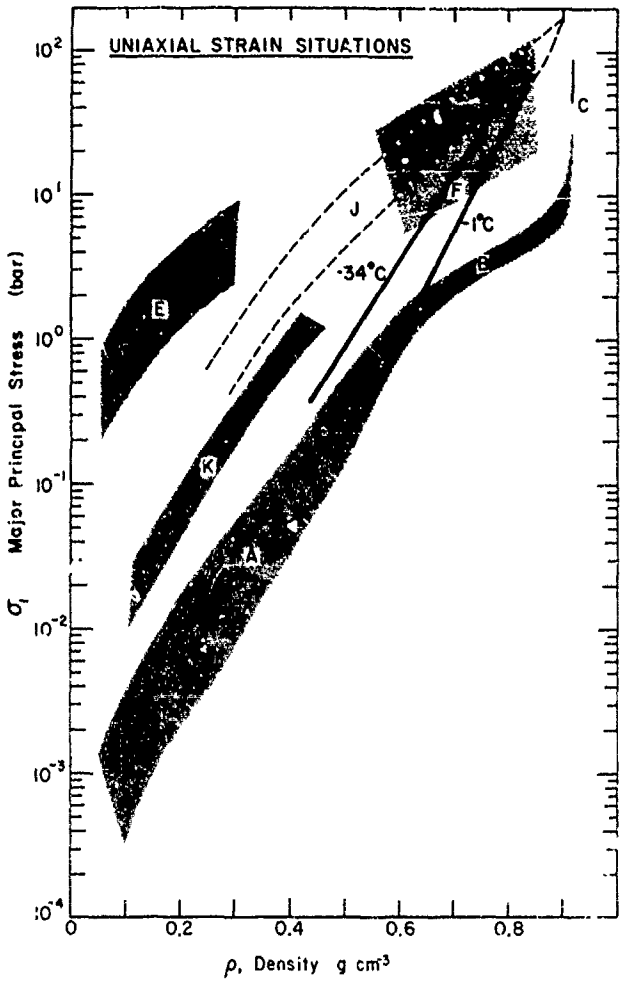

A: *Natural densification of snow deposits, -1° to -48°C. Approximate average loading rates 10^{-10} to 10^{-8} bar/s.* B: *Slow natural compression of dense firn and porous ice (from depth/density curves for polar ice caps).* C: *Slow compression of solid ice.* E: *Calculated values for plane wave impact at 20 to 40 m/s.* F: *Hugoniot data for explosively generated shock waves (impact velocities 1 to 12 m/s), -7° to -18°C.* J: *Compression at approximately constant strain rate, -7° to -18°C. Strain rate ≈ 10^{-4} s^{-1}.* K: *Compression in uniaxial strain — incremental loading to collapse, -2° to -3°C.*

Figure 35. Yield envelopes for compacted snow compared with various stress-density data.

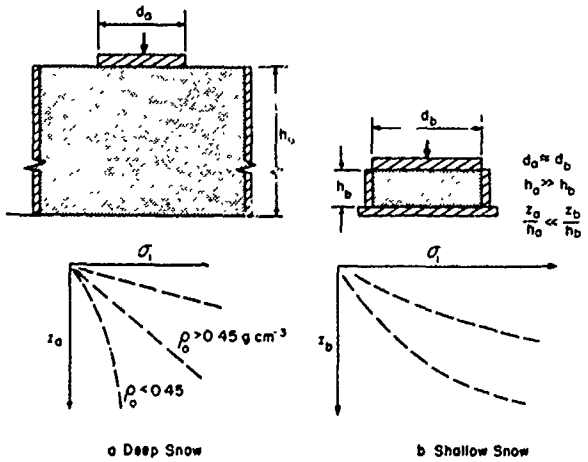

Figure 36. Comparison of stress-deformation relationships for two different test conditions, where σ_1 is the principal stress, d the sample diameter, h the sample height, and z the vertical deformation.

MICROSTRUCTURAL EXAMINATION OF ARTIFICIALLY COMPACTED SNOW

Any appreciable compression of snow will produce some crushing of the individual snow grains. At higher compressive stresses this crushing will also be accompanied by significant changes in the size, shape and orientation of the constituent grains and/or crystals. Studies conducted by Abele and Gow (1975) demonstrated that the extent to which artifically compacted snow recrystallized increased with both an increase in the compactive pressure and the temperature, especially as temperatures approached 0°C. This earlier work also indicated that a significant transition in the physical and mechanical properties of compacted snow may occur at about -10°C. A principal objective of the present study was to determine if a crystal structure transition also exists at or near this temperature.

Analytical techniques

The techniques used to investigate snow structure were essentially the same as those described by Abele and Gow (1975). The basic method involves impregnating the permeable snow sample with water-saturated aniline to facilitate the mounting of the sample on a glass slide, and then sectioning the aniline-filled sample with the aid of a microtome. Analysis of the thin section is most conveniently accomplished with photomicrographs obtained with a Bausch and Lomb bellows camera fitted with polarizers. Full details of this technique are to be found in Gow (1969).

Results and discussion

Examination of structure was confined to samples tested at two stress levels at temperatures of -1°, -10° and -34°C. Structural characteristics of some representative compacts are illustrated in Figure 37.

None of the samples tested at the lower stress (26-29 bars) attained densities in excess of 0.72 g cm^{-3}. Of these the highest values were only obtained with samples that had been precompacted to more than 0.50 g cm^{-3}. The microstructural characteristics of these samples are compatible with appreciable crushing of grains and incipient recrystallization of the kind that leads to substantial rounding of grain outlines but little growth of crystals. The sizes of grains averaged only about 0.2 mm in diameter. All samples possessed an open bubble structure that was thoroughly permeable to aniline. The structure of the original snow is demonstrated in Figure 37; it is composed mainly of broken crystals and angular particles that frequently clump together in clusters.

All samples compacted at the higher stress (70-72 bars) possessed ice-like texture, though from density considerations only the -1°C compact (sample 43) could be said to have recrystallized to ice *per se*. The density of ice is generally set at values greater than 0.82 g cm^{-3}, at which density the compacted sample is no longer permeable, though it may still contain abundant numbers of disconnected air bubbles.

The crystal-bubble relationships of the -1°C compact (sample 43) are essentially the same as those obtained under similar conditions in the tests conducted earlier by Abele and Gow (1975). The texture is composed largely of equidimensional grains which frequently intersect one another at equilibrium angles of 120°. This condition would suggest that substantially complete post-deformational recrystallization has occurred in this particular compact. The mean crystal diameter is about 0.5 mm. Entrapped air bubbles are composed mainly of squat, tubular and well-rounded inclusions that do not usually exceed 0.1 mm in diameter. The porosity of sample 43 cannot exceed 1% and additional tests indicate that the gas contained in the bubbles is under some pressure. The pore-crystal relationships in sample 43 simulate very closely those observed in hot-pressed compacts of metallic powders.

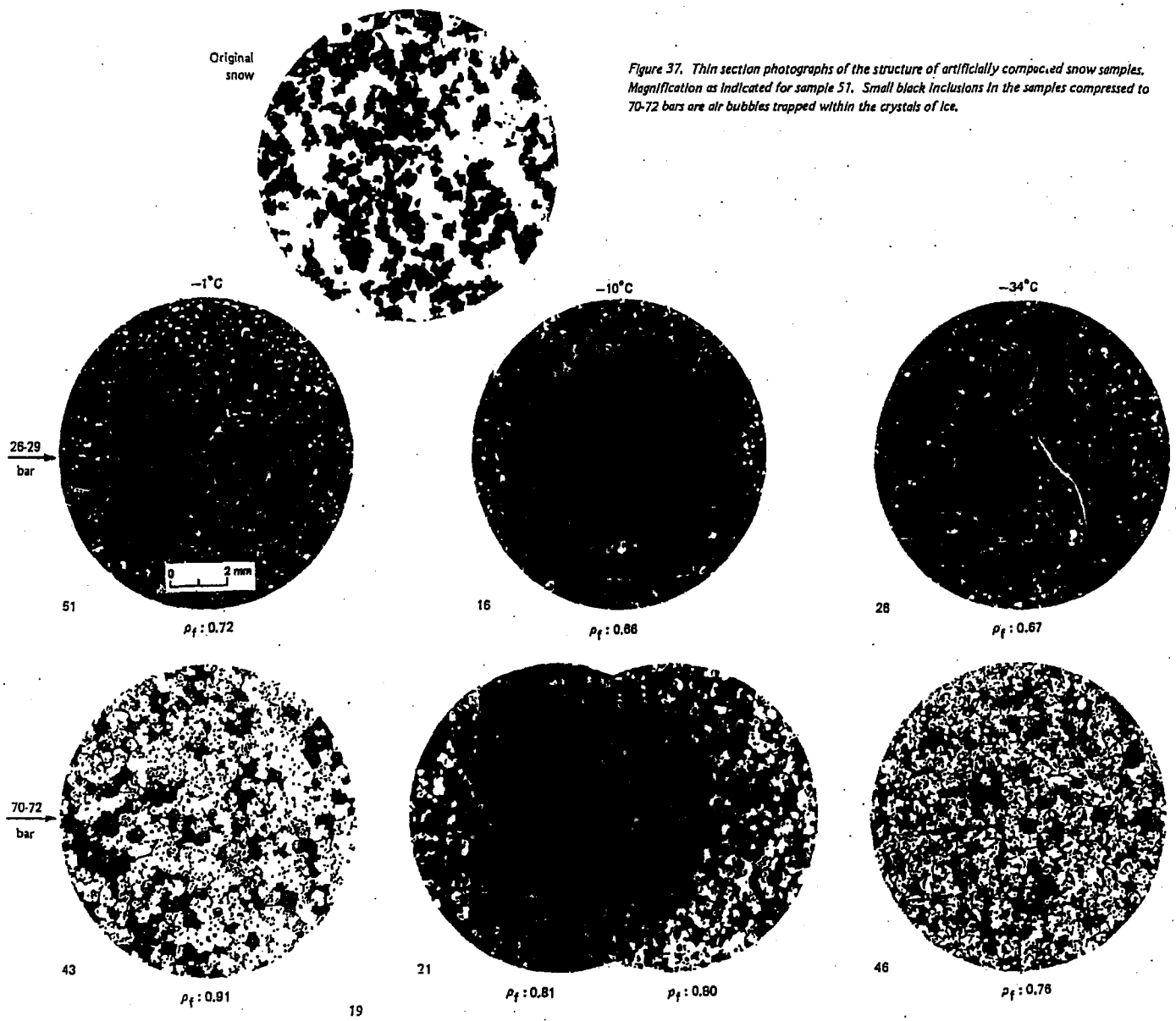

Figure 37. Thin section photographs of the structure of artificially compacted snow samples. Magnification as indicated for sample 51. Small black inclusions in the samples compressed to 70-72 bars are air bubbles trapped within the crystals of ice.

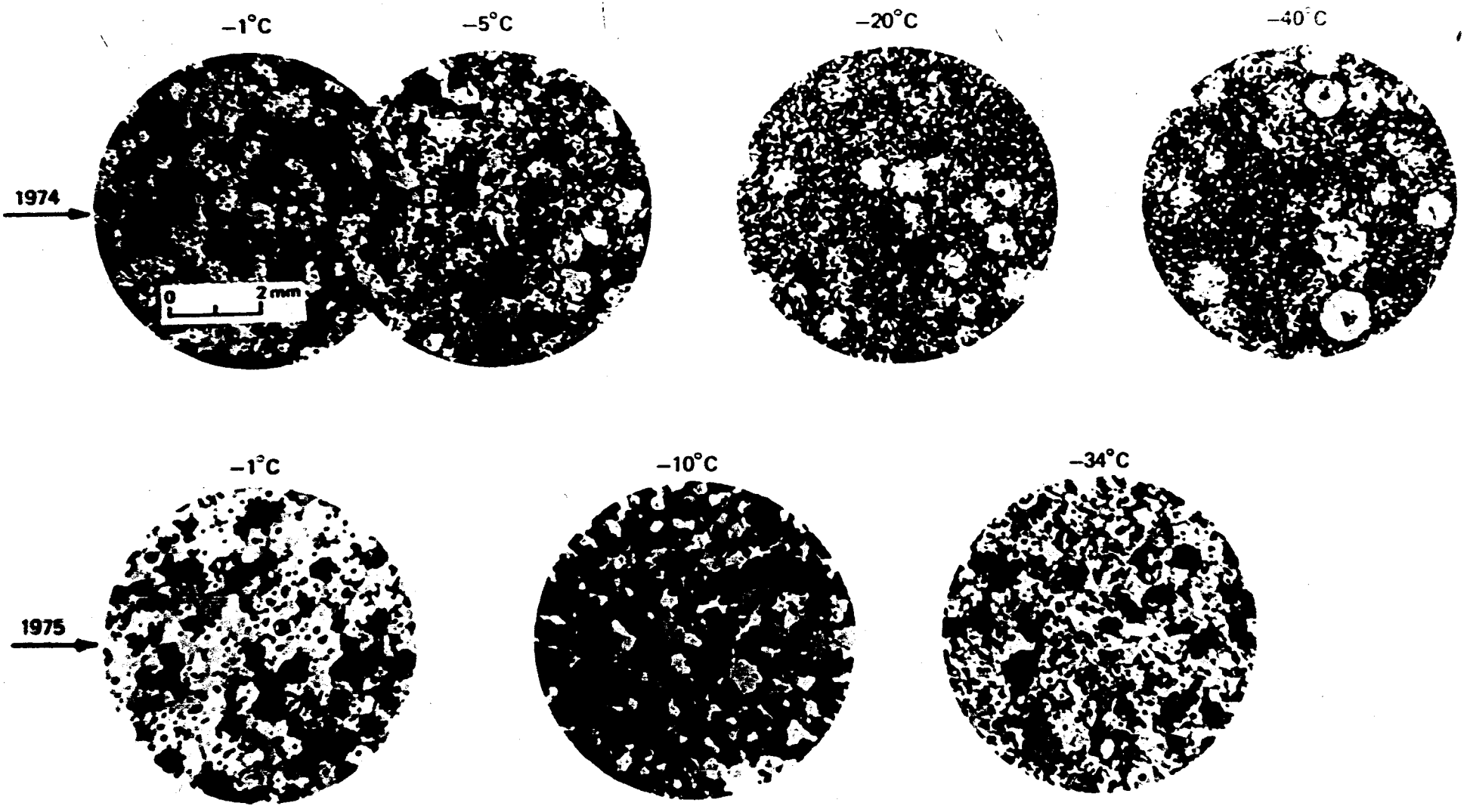

Figure 38. Photomicrographs illustrating variable recrystallization in two separate series compacted at 70-75 bars at the temperatures indicated.

The density of sample 21, tested at -10°C, is very close to that of ice, and the textural properties of this particular specimen, as observed in thin section (Fig. 37), certainly confirm the dense condition of this compact. This particular compact contains abundant rounded bubbles of approximately the same dimensions at those in sample 43, but the constituent crystals in sample 21 are very much smaller. This condition is even more apparent from a comparison with the textural characteristics of sample 46, tested at -34°C. Whereas the crystalline structure of sample 46 still bears the imprint of incomplete recrystallization (crystal boundaries are imperfectly developed in many instances), the sizes of the crystals are measurably larger than in sample 21. The unusually fine-grained nature of sample 21 is not peculiar just to this particular specimen; two additional samples tested under identical conditions (compacted to 72 bars at -10°C) also yielded essentially identical textures. Just why the crystal size of the -10°C compact should be significantly smaller than that tested at -34°C is not known, especially since both sets of samples were prepared from the same parent material. We can only suspect that post-deformational crystallization is in some way involved, and that this has led to a larger grain size in the -34°C test piece. However, it should be emphasized that apart from its smaller size of grain, the texture of the -10°C compact is still much more extensively recrystallized. The larger grain size in sample 46 might be linked to the fact that all samples were returned to the -8°C coldroom for density measurements, and this substantial elevating of the temperature of sample 46 following testing could have promoted the growth of larger crystals.

A comparison of this year's studies by Abele and Gow (1975) (Fig. 38) demonstrates that the course of recrystallization can vary appreciably in two separate sets of samples subjected to much the same test conditions. In the earlier tests at the highest stresses, all samples compacted at temperatures of -5°C and colder were characterized by growth of a few large crystals in a fine-grained matrix. It would seem in this particular set of samples that the energy of recrystallization was concentrated at just a few scattered locations within the deformed matrix. In this year's tests, on the other hand, it would appear that post-deformational recrystallization has led to the formation of textures of more uniform grain size within the deformed matrix.

Conclusions

This study confirms the earlier work of Abele and Gow (1975) that the compaction of snow can lead to extensive recrystallization of the deformed aggegate. However, the nature of the recrystallization, especially the crystal growth factor, can vary with different sets of samples tested under similar conditions. The exact reasons for these variations in the course of recrystallization are not completely understood, though small differences in test procedure, purity of the parent snow and temperature history of the compacted sample are probably all involved. At the nominal pressure of 70-75 bars it would appear that the transformation to ice ceases at some temperature between -5°C and -10°C. This transformation is not clearly reflected in the recrystallization textures.

LITERATURE CITED

Abele, G. (1970) Deformation of snow under rigid plates at a constant rate of deformation. USA CRREL Research Report 273. AD 704708.

Abele, G. and A.J. Gow (1975) Compressibility characteristics of undisturbed snow. USA CRREL Research Report 336.

Assur, A. (1964) Locomotion over soft soil and snow. *Proceedings, Automotive Engineering Congress*, Detroit, Michigan, no. 782F.

Gow, A.J. (1969) On the rates of growth of grains and crystals in south polar firn. *Journal of Glaciology*, vol. 8, no. 53, p. 241-252.

Mellor, M. (1974) A review of basic snow mechanics. *Proceedings, International Symposium on Snow Mechanics, International Commission of Snow and Ice*, IUGG, Grindelwald, Switzerland.

APPENDIX: PHOTOGRAPHS OF OSCILLOSCOPE TRACES

NOMENCLATURE

T	Temperature
d	Sample diameter
h_0	Initial sample height
h_f	Sample height after compression
A	Sample area
V_0	Initial sample volume
V_f	Sample volume after compression
W	Sample weight
ρ_0	Initial sample density
ρ_f	Sample density after compression

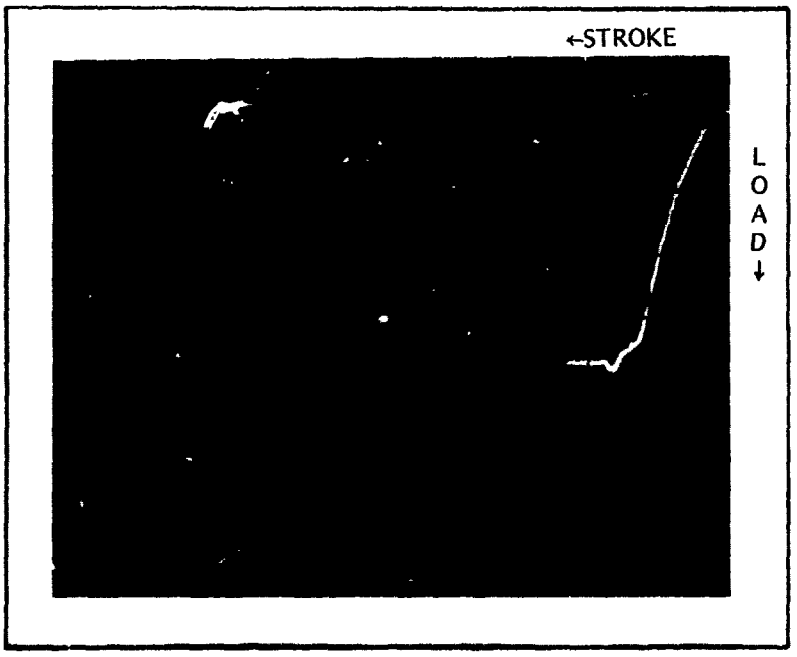

Date: 24Feb75

Sample

Snow type: 2 hrs

T	(^oC)	= -1
d	(cm)	= 12.7
h_o	(cm)	= 5.1
A	(cm^2)	= 126.6
V_o	(cm^3)	= 643
W	(g)	= 407
ρ_o	(gcm^{-3})	= .634
h_f	(cm)	= 3.60
V_f	(cm^3)	= 456
ρ_f	(gcm^{-3})	= .893

Test No. 1 Rate of deform. ($cm\ sec^{-1}$) = 40

Load: Vert. scale: 1 div. = 2275 (kg)
Stroke: Horiz. scale: 1 div. = 0.64 (cm)

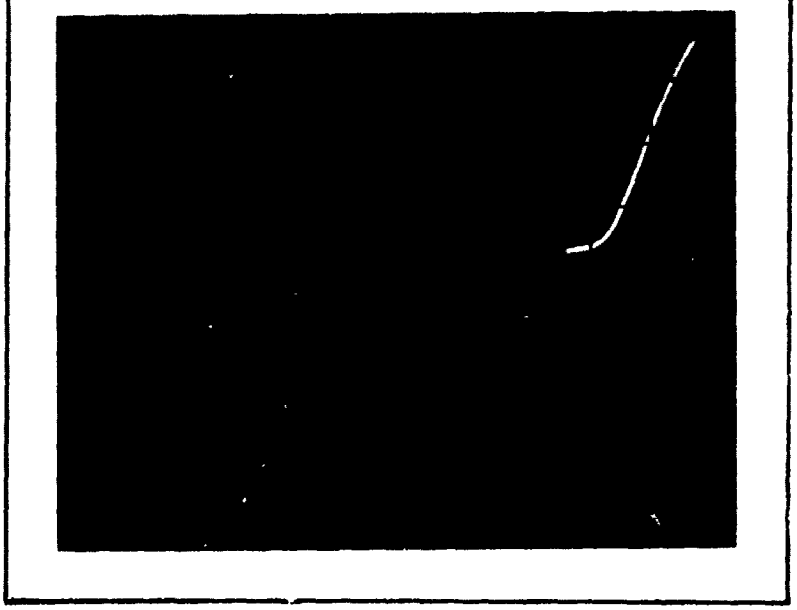

Date: 24Feb75

Sample

Snow type: 2 hrs

T	(^oC)	= -1
d	(cm)	= 12.7
h_o	(cm)	= 5.1
A	(cm^2)	= 126.6
V_o	(cm^3)	= 643
W	(g)	= 430
ρ_o	(gcm^{-3})	= .669
h_f	(cm)	= 3.75
V_f	(cm^3)	= 474
ρ_f	(gcm^{-3})	= .907

Test No. 4 Rate of deform. ($cm\ sec^{-1}$) = 40

Load: Vert. scale: 1 div. = 2275 (kg)
Stroke: Horiz. scale: 1 div. = 0.64 (cm)

CRREL Form 42 (OT)
15 May 74

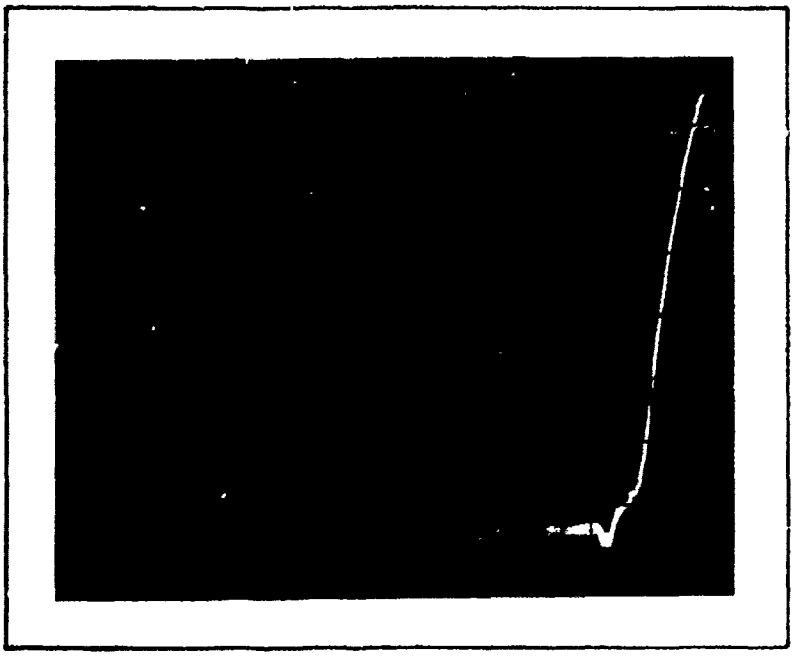

Date: 24 Feb 75

Sample

Snow type: 2 hrs

T	(^{o}C)	= -1
d	(cm)	= 12.7
h_o	(cm)	= 5.1
A	(cm^2)	= 126.6
V_o	(cm^3)	= 643
W	(g)	= 426
ρ_o	(gcm^{-3})	= .663
h_f	(cm)	= 3.70
V_f	(cm^3)	= 468
ρ_f	(gcm^{-3})	= .91

Test No. 5 Rate of deform. ($cm\ sec^{-1}$) = 40

Load: Vert. scale: 1 div. = 1138 (kg)
Stroke: Horiz. scale: 1 div. = 0.64 (cm)

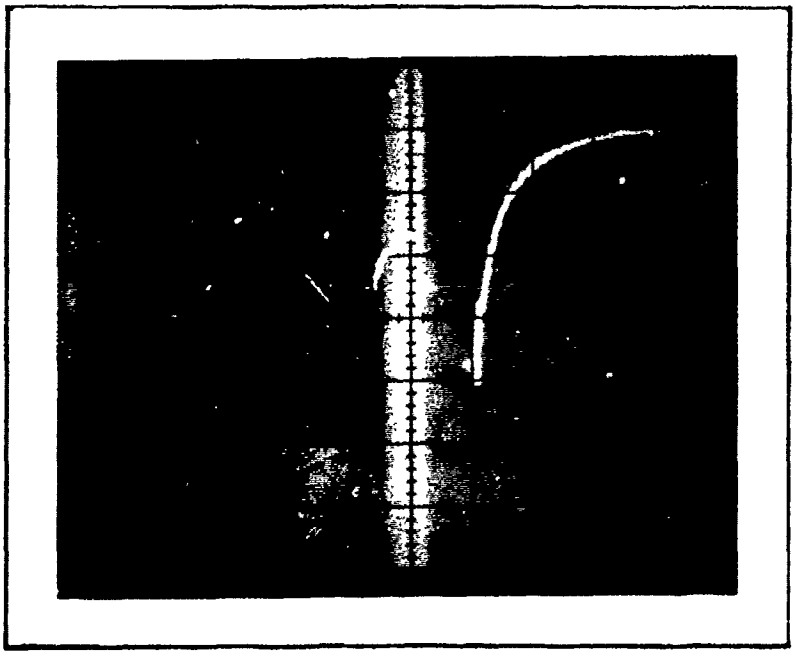

Date: 3 Mar 75

Sample

Snow type: 2 hrs

T	(^{o}C)	= -10
d	(cm)	= 12.7
h_o	(cm)	= 5.1
A	(cm^2)	= 126.6
V_o	(cm^3)	= 643
W	(g)	= 326
ρ_o	(gcm^{-3})	= .507
h_f	(cm)	= 3.0
V_f	(cm^3)	= 380
ρ_f	(gcm^{-3})	= .858

Test No. 6 Rate of deform. ($cm\ sec^{-1}$) = 40

Load: Vert. scale: 1 div. = 2275 (kg)
Stroke: Horiz. scale: 1 div. = 0.64 (cm)

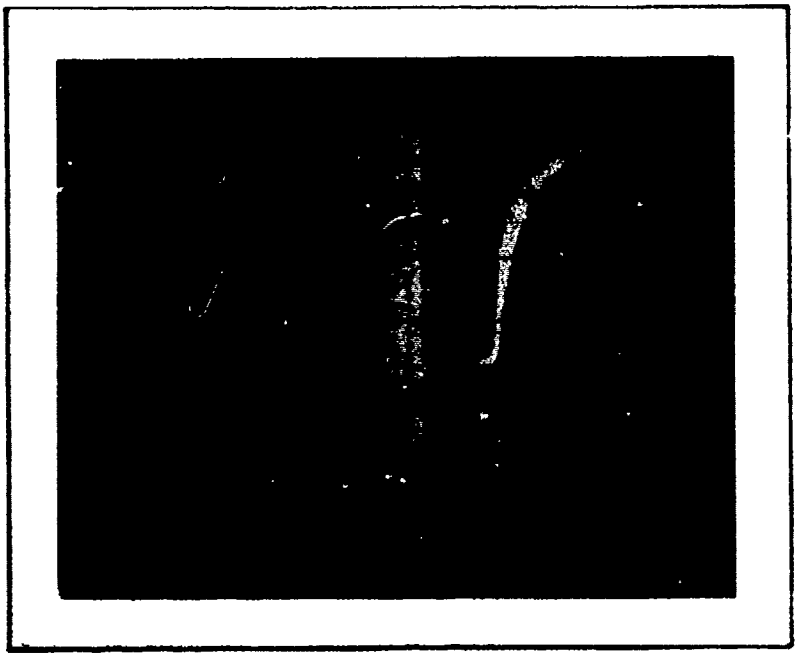

Date: 3 Mar 75

Sample

Snow type: 2 hrs

T	(^{o}C)	= -10
d	(cm)	= 12.7
h_o	(cm)	= 5.1
A	(cm^2)	= 126.6
V_o	(cm^3)	= 643
W	(g)	= 333
ρ_o	(gcm^{-3})	= .518
h_f	(cm)	= 3.10
V_f	(cm^3)	= 392
ρ_f	(gcm^{-3})	= .850

Test No. 7 Rate of deform. ($cm\ sec^{-1}$) = 40

Load: Vert. scale: 1 div. = 2275 (kg)
Stroke: Horiz. scale: 1 div. = 0.64 (cm)

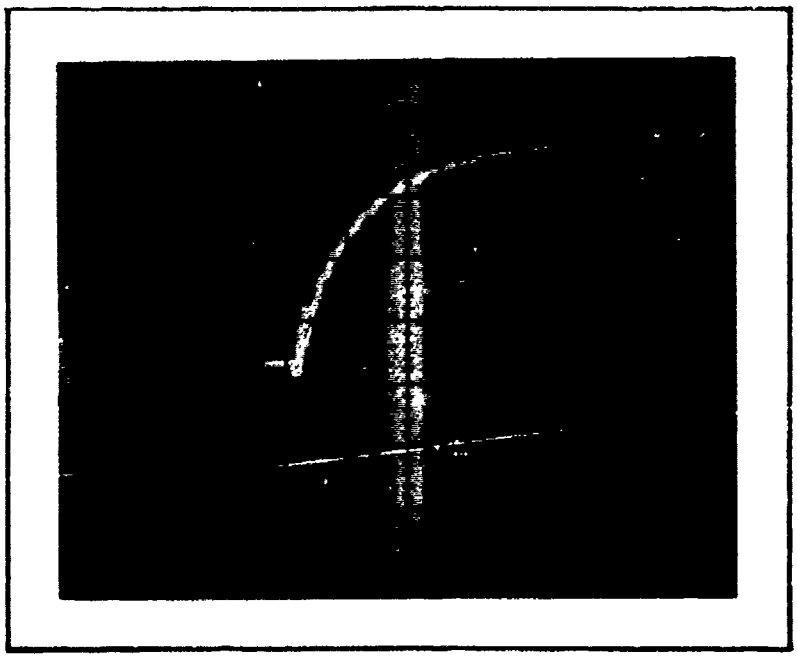

Date: 3 Mar 75

Sample

Snow type: 2 hrs

T	(^{o}C)	= -10
d	(cm)	= 12.7
h_o	(cm)	= 5.1
A	(cm^2)	= 126.6
V_o	(cm^3)	= 643
W	(g)	= 341
ρ_o	(gcm^{-3})	= .531
h_f	(cm)	= 3.10
V_f	(cm^3)	= 392
ρ_f	(gcm^{-3})	= .870

Test No. 8 Rate of deform. ($cm\ sec^{-1}$) = 40

Load: Vert. scale: 1 div. = 2275 (kg)
Stroke: Horiz. scale: 1 div. = 0.25 (cm)

CRREL Form 42 (OT)
15 May 74

Date: 3 Mar 75

Sample

Snow type: 2 hrs

T	(°C)	= -10
d	(cm)	= 12.7
h_o	(cm)	= 5.1
A	(cm^2)	= 126.6
V_o	(cm^3)	= 643
W	(g)	= 332
ρ_o	(gcm^{-3})	= .516
h_f	(cm)	= 3.10
V_f	(cm^3)	= 392
ρ_f	(gcm^{-3})	= .847

Test No. 9 Rate of deform. ($cm\ sec^{-1}$) = 40

Load: Vert. scale: 1 div. = 2275 (kg)
Stroke: Horiz. scale: 1 div. = 0.25 (cm)

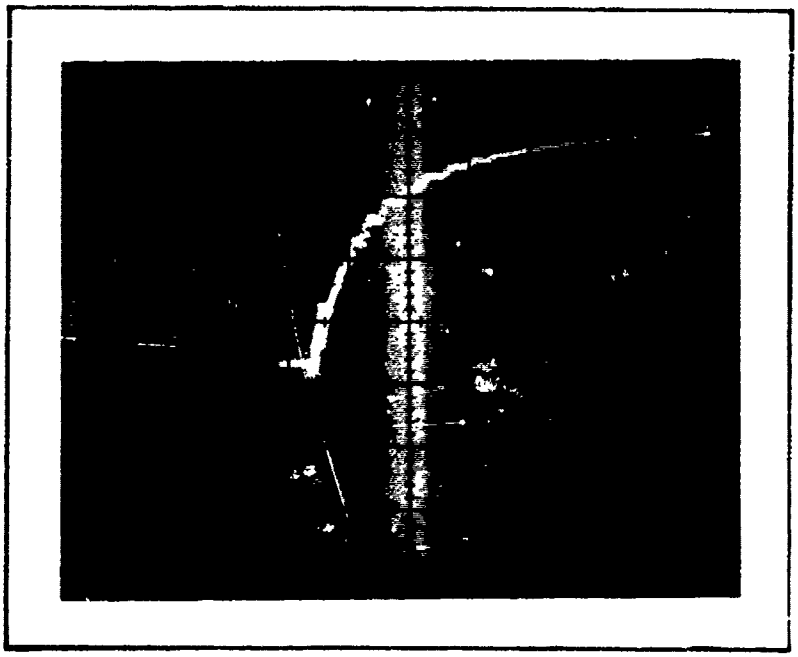

Date: 3 Mar 75

Sample

Snow type: 2 hrs

T	(°C)	= -10
d	(cm)	= 12.7
h_o	(cm)	= 5.1
A	(cm^2)	= 126.6
V_o	(cm^3)	= 643
W	(g)	= 326
ρ_o	(gcm^{-3})	= .507
h_f	(cm)	= 3.0
V_f	(cm^3)	= 380
ρ_f	(gcm^{-3})	= .858

Test No. 10 Rate of deform. ($cm\ sec^{-1}$) = 40

Load: Vert. scale: 1 div. = 2275 (kg)
Stroke: Horiz. scale: 1 div. = 0.25 (cm)

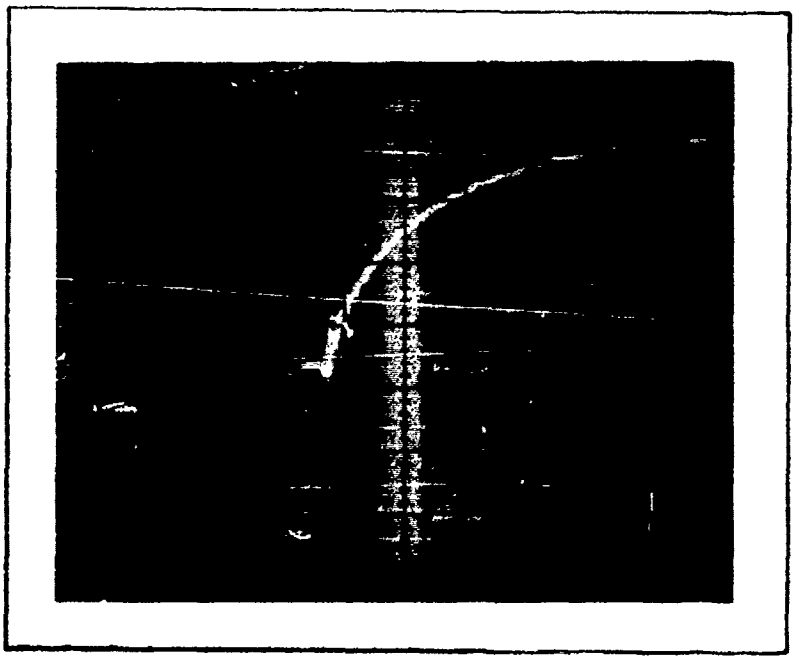

Date: 3 Mar 75

Sample

Snow type: 2 hrs

T	(°C)	= -10
d	(cm)	= 20.3
h_o	(cm)	= 5.1
A	(cm^2)	= 323.3
V_o	(cm^3)	= 1633
W	(g)	= 811
ρ_o	(gcm^{-3})	= .496
h_f	(cm)	= 3.25
V_f	(cm^3)	= 1050
ρ_f	(gcm^{-3})	= .772

Test No. 11 Rate of deform. ($cm\ sec^{-1}$) = 40

Load: Vert. scale: 1 div. = 2275 (kg)
Stroke: Horiz. scale: 1 div. = 0.25 (cm)

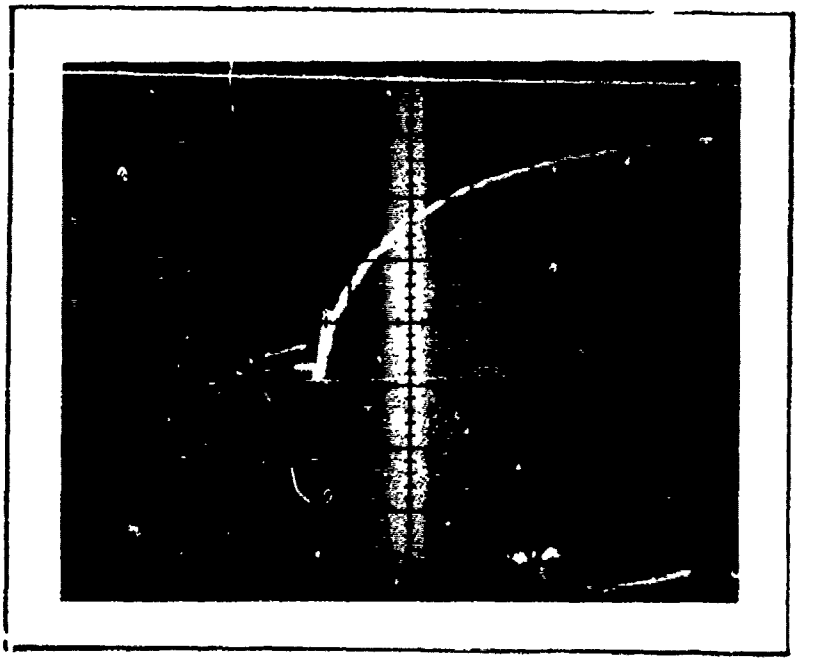

Date: 3 Mar 75

Sample

Snow type: 2 hrs

T	(°C)	= -10
d	(cm)	= 20.3
h_o	(cm)	= 5.1
A	(cm^2)	= 323.3
V_o	(cm^3)	= 1633
W	(g)	= 819
ρ_o	(gcm^{-3})	= .501
h_f	(cm)	= 3.30
V_f	(cm^3)	= 1066
ρ_f	(gcm^{-3})	= .769

Test No. 12 Rate of deform. ($cm\ sec^{-1}$) = 40

Load: Vert. scale: 1 div. = 2275 (kg)
Stroke: Horiz. scale: 1 div. = 0.25 (cm)

CRREL Form 42 (OT)
15 May 74

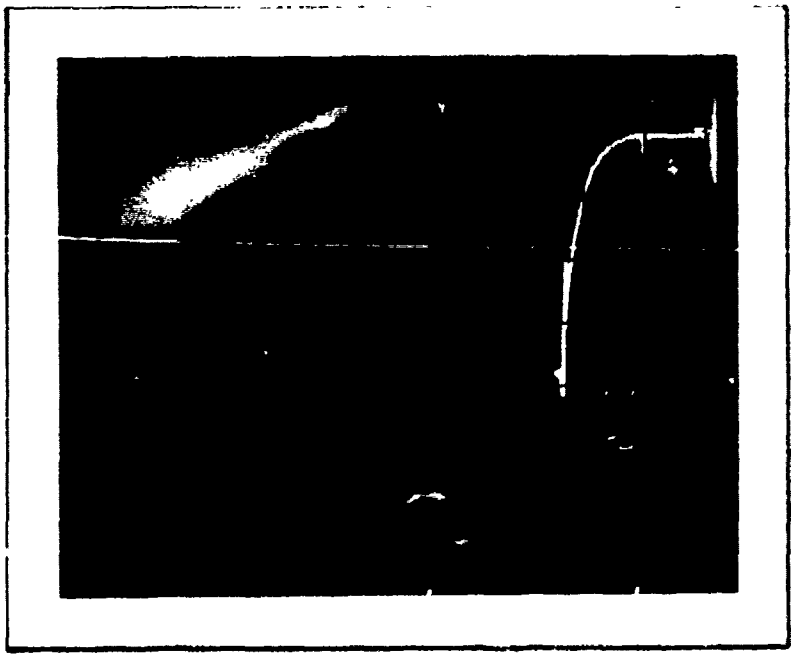

Date: 14 Mar 75

Sample

Snow type: 7 days

T	(°C)	= -10
d	(cm)	= 20.3
h_o	(cm)	= 5.1
A	(cm^2)	= 323.3
V_o	(cm^3)	= 1633
W	(g)	= 471
ρ_o	(gcm^{-3})	= .288
h_f	(cm)	= 2.12
V_f	(cm^3)	= 685
ρ_f	(gcm^{-3})	= .688

Test No. 13 Rate of deform. ($cm\ sec^{-1}$) = 40

Load: Vert. scale: 1 div. = 2275 (kg)
Stroke: Horiz. scale: 1 div. = 1.27 (cm)

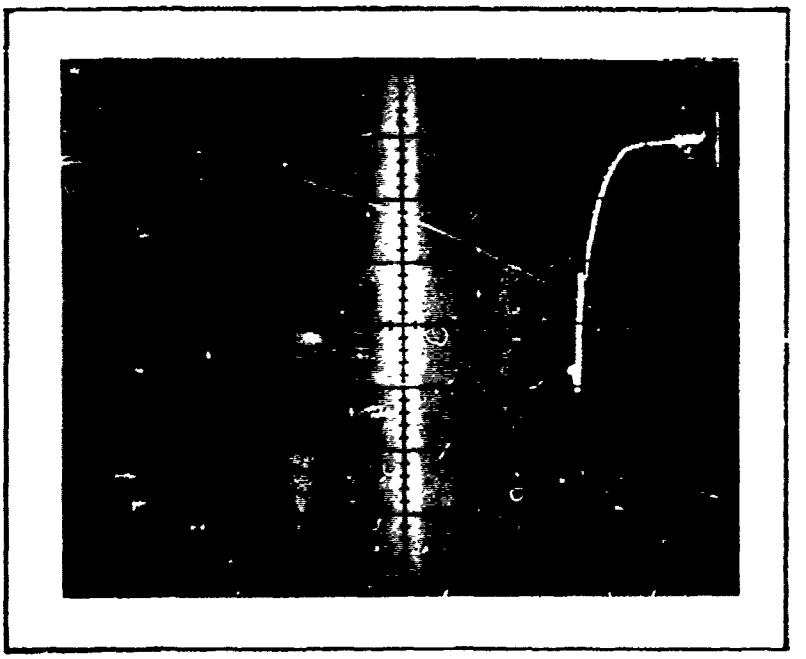

Date: 14 Mar 75

Sample

Snow type: 7 days

T	(°C)	= -10
d	(cm)	= 20.3
h_o	(cm)	= 5.1
A	(cm^2)	= 323.3
V_o	(cm^3)	= 1633
W	(g)	= 542
ρ_o	(gcm^{-3})	= .332
h_f	(cm)	= 2.45
V_f	(cm^3)	= 792
ρ_f	(gcm^{-3})	= .685

Test No. 14 Rate of deform. ($cm\ sec^{-1}$) = 40

Load: Vert. scale: 1 div. = 2275 (kg)
Stroke: Horiz. scale: 1 div. = 1.27 (cm)

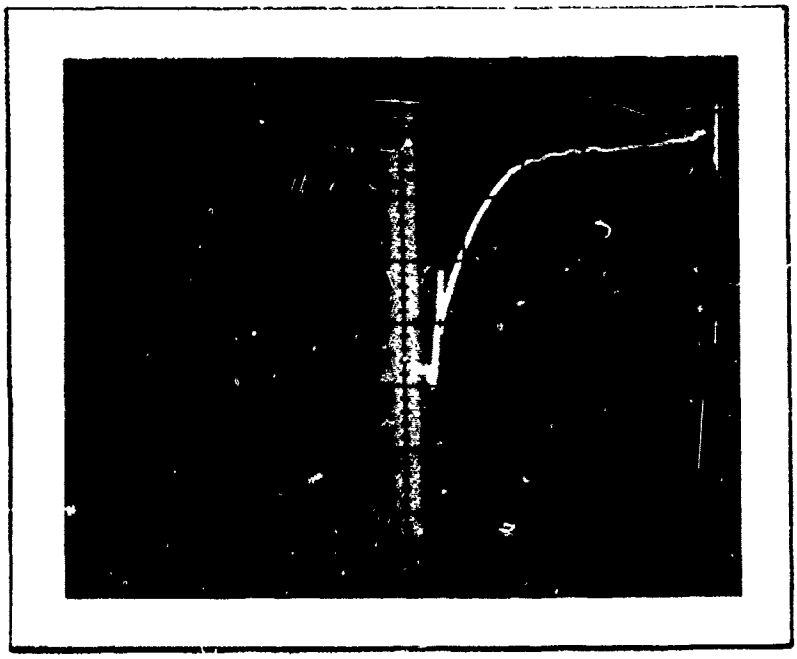

Date: 14 Mar 75

Sample

Snow type: 7 days

T	(°C)	= -10
d	(cm)	= 20.3
h_o	(cm)	= 5.1
A	(cm^2)	= 323.3
V_o	(cm^3)	= 1633
W	(g)	= 607
ρ_o	(gcm^{-3})	= .372
$h_{\frac{1}{4}}$	(cm)	= 2.70
$V_{\frac{1}{4}}$	(cm^3)	= 873
$\rho_{\frac{1}{4}}$	(gcm^{-3})	= .695

Test No. 15 Rate of deform. ($cm\ sec^{-1}$) = 40

Load: Vert. scale: 1 div. = 2.275 (kg)
Stroke: Horiz. scale: 1 div. = 0.51 (cm)

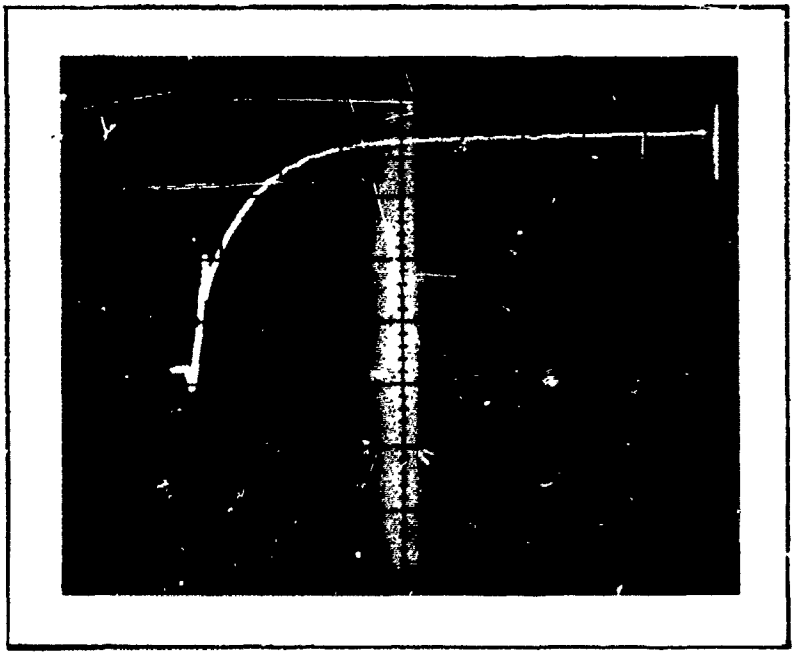

Date: 14 Mar 75

Sample

Snow type: 7 days

T	(°C)	= -10
d	(cm)	= 20.3
h_o	(cm)	= 7.6
A	(cm^2)	= 323.3
V_o	(cm^3)	= 2460
W	(g)	= 696
ρ_o	(gcm^{-3})	= .283
$h_{\frac{1}{4}}$	(cm)	= 3.25
$V_{\frac{1}{4}}$	(cm^3)	= 1050
$\rho_{\frac{1}{4}}$	(gcm^{-3})	= .663

Test No. 16 Rate of deform. ($cm\ sec^{-1}$) = 40

Load: Vert. scale: 1 div. = 2.275 (kg)
Stroke: Horiz. scale: 1 div. = 0.51 (cm)

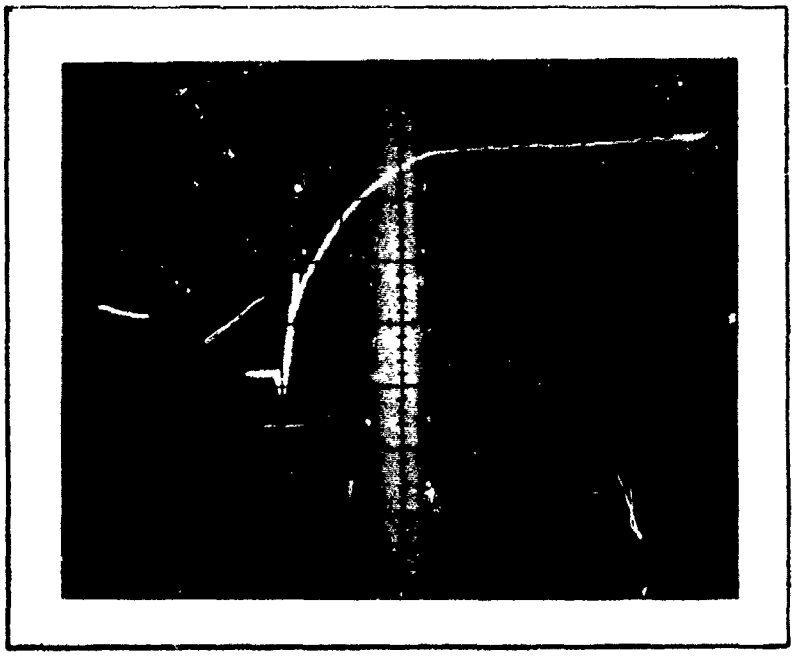

Date: 14 Mar 75

Sample

Snow type: 7 days

T	(^{o}C)	= -10
d	(cm)	= 20.3
h_o	(cm)	= 7.6
A	(cm^2)	= 323.3
V_o	(cm^3)	= 2460
W	(g)	= 855
ρ_o	(gcm^{-3})	= .348
h_f	(cm)	= 4.0
V_f	(cm^3)	= 1291
ρ_f	(gcm^{-3})	= .662

Test No. 17 Rate of deform. ($cm\ sec^{-1}$) = 40

Load: Vert. scale: 1 div. = 2275 (kg)
Stroke: Horiz. scale: 1 div. = 0.51 (cm)

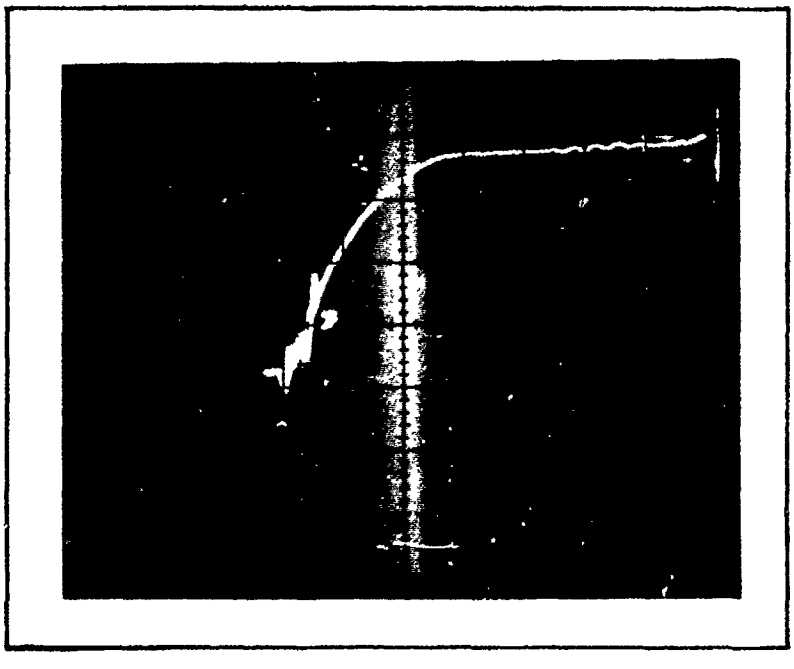

Date: 14 Mar 75

Sample

Snow type: 7 days

T	(^{o}C)	= -10
d	(cm)	= 20.3
h_o	(cm)	= 7.6
A	(cm^2)	= 323.3
V_o	(cm^3)	= 2460
W	(g)	= 849
ρ_o	(gcm^{-3})	= .345
h_f	(cm)	= 3.95
V_f	(cm^3)	= 1275
ρ_f	(gcm^{-3})	= .665

Test No. 18 Rate of deform. ($cm\ sec^{-1}$) = 40

Load: Vert. scale: 1 div. = 2275 (kg)
Stroke: Horiz. scale: 1 div. = 0.51 (cm)

CRREL Form 42 (OT)
15 May 74

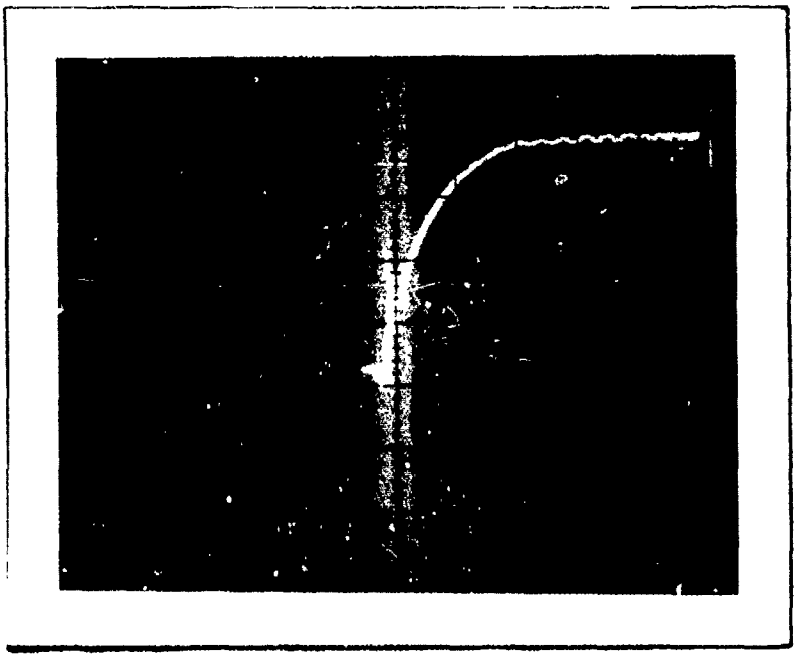

Date: 14 Mar 75

Sample

Snow type: 7 days

T	(^{o}C)	= -10
d	(cm)	= 12.7
h_o	(cm)	= 5.1
A	(cm^2)	= 126.6
V_o	(cm^3)	= 643
W	(g)	= 222
ρ_o	(gcm^{-3})	= .346
h_f	(cm)	= 2.20
V_f	(cm^3)	= 278
ρ_f	(gcm^{-3})	= .798

Test No. 19 Rate of deform. ($cm\ sec^{-1}$) = 40

Load: Vert. scale: 1 div. = 2275 (kg)
Stroke: Horiz. scale: 1 div. = 0.51 (cm)

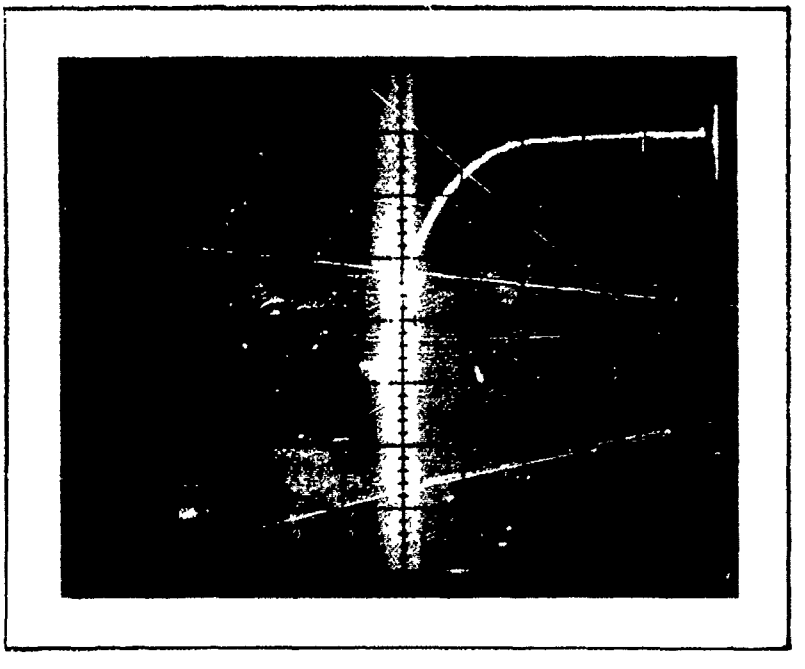

Date: 14 Mar 75

Sample

Snow type: 7 days

T	(^{o}C)	= -10
d	(cm)	= 12.7
h_o	(cm)	= 5.1
A	(cm^2)	= 126.6
V_o	(cm^3)	= 643
W	(g)	= 223
ρ_o	(gcm^{-3})	= .347
h_f	(cm)	= 2.20
V_f	(cm^3)	= 278
ρ_f	(gcm^{-3})	= .802

Test No. 20 Rate of deform. ($cm\ sec^{-1}$) = 40

Load: Vert. scale: 1 div. = 2275 (kg)
Stroke: Horiz. scale: 1 div. = 0.51 (cm)

CRREL Form 42 (OT)
15 May 74

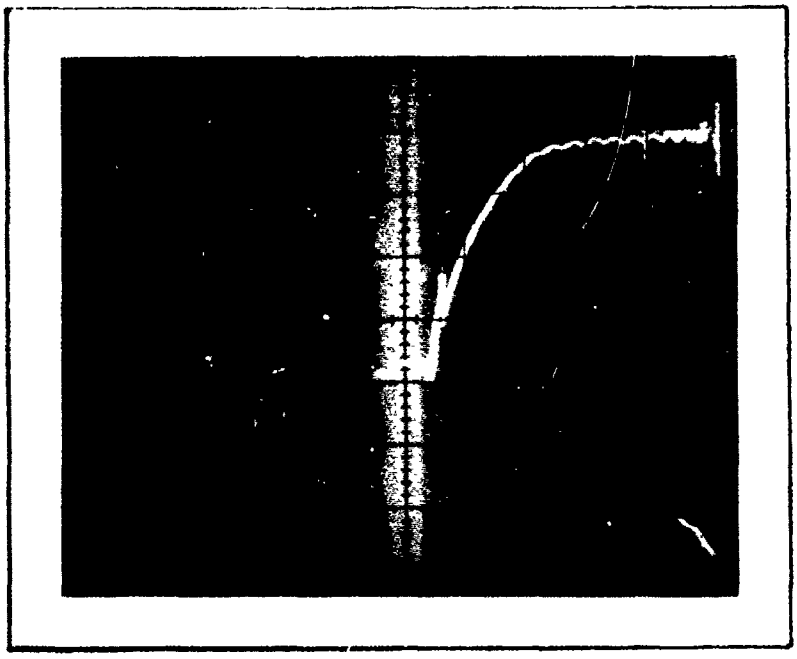

Date: 14 Mar 75

Sample

Snow type: 7 days

T	(°C)	= -10
d	(cm)	= 12.7
h_o	(cm)	= 5.1
A	(cm^2)	= 126.6
V_o	(cm^3)	= 643
W	(g)	= 256
ρ_o	(gcm^{-3})	= .398
h_f	(cm)	= 2.50
V_f	(cm^3)	= 316
ρ_f	(gcm^{-3})	= .810

Test No. 21 Rate of deform. ($cm\ sec^{-1}$) = 40

Load: Vert. scale: 1 div. = 2275 (kg)
Stroke: Horiz. scale: 1 div. = 0.51 (cm)

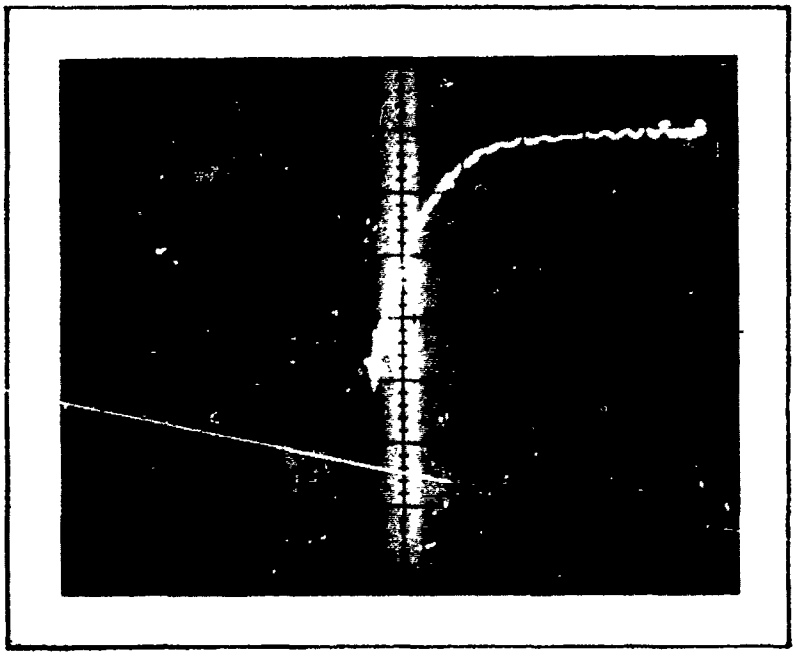

Date: 14 Mar 75

Sample

Snow type: 7 days

T	(°C)	= -34
d	(cm)	= 12.7
h_o	(cm)	= 5.1
A	(cm^2)	= 126.6
V_o	(cm^3)	= 643
W	(g)	= 221
ρ_o	(gcm^{-3})	= .344
h_f	(cm)	= 2.30
V_f	(cm^3)	= 291
ρ_f	(gcm^{-3})	= .760

Test No. 22 Rate of deform. ($cm\ sec^{-1}$) = 40

Load: Vert. scale: 1 div. = 2275 (kg)
Stroke: Horiz. scale: 1 div. = 0.51 (cm)

CRREL Form 42 (OT)
15 May 74

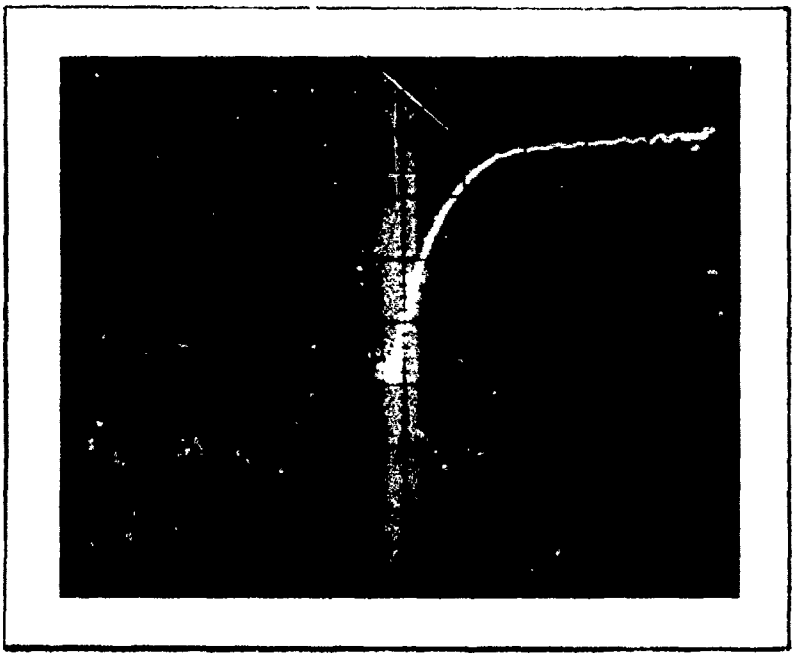

Date: 14 Mar 75

Sample

Snow type: 7 days

T	(°C)	= -34
d	(cm)	= 12.7
h_o	(cm)	= 5.1
A	(cm^2)	= 126.6
V_o	(cm^3)	= 643
W	(g)	= 232
ρ_o	(gcm^{-3})	= .361
h_f	(cm)	= 2.40
V_f	(cm^3)	= 304
ρ_f	(gcm^{-3})	= .764

Test No. 23 Rate of deform. ($cm\ sec^{-1}$) = 40

Load: Vert. scale: 1 div. = 2275 (kg)
Stroke: Horiz. scale: 1 div. = 0.51 (cm)

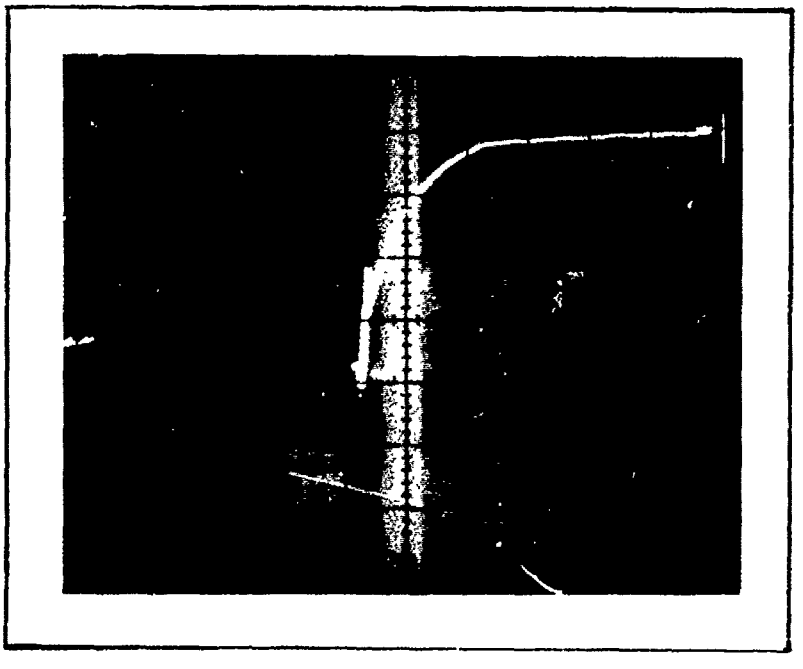

Date: 14 Mar 75

Sample

Snow type: 7 days

T	(°C)	= -34
d	(cm)	= 20.3
h_o	(cm)	= 5.1
A	(cm^2)	= 323.3
V_o	(cm^3)	= 1633
W	(g)	= 486
ρ_o	(gcm^{-3})	= .301
h_f	(cm)	= 2.30
V_f	(cm^3)	= 743
ρ_f	(gcm^{-3})	= .655

Test No. 24 Rate of deform. ($cm\ sec^{-1}$) = 40

Load: Vert. scale: 1 div. = 2275 (kg)
Stroke: Horiz. scale: 1 div. = 0.51 (cm)

CRREL Form 42 (OT)
15 May 74

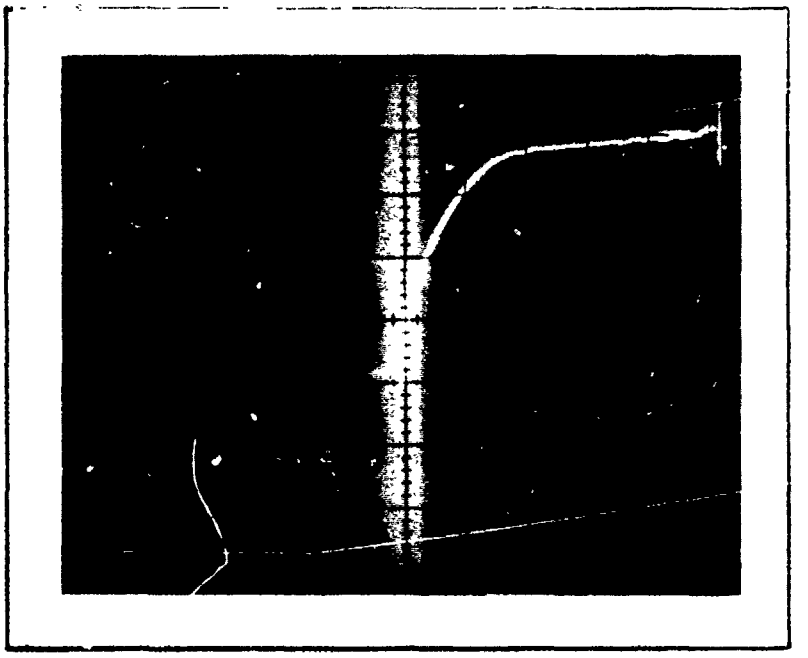

Date: 14 Mar 75

Sample

Snow type: 7 days

T	(°C)	= -34
d	(cm)	= 20.3
h_o	(cm)	= 5.1
A	(cm^2)	= 323.3
V_o	(cm^3)	= 1633
W	(g)	= 535
ρ_o	(gcm^{-3})	= .328
h_f	(cm)	= 2.55
V_f	(cm^3)	= 824
ρ_f	(gcm^{-3})	= .650

Test No. 25 Rate of deform. ($cm\ sec^{-1}$) = 40

Load: Vert. scale: 1 div. = 2275 (kg)
Stroke: Horiz. scale: 1 div. = 0.51 (cm)

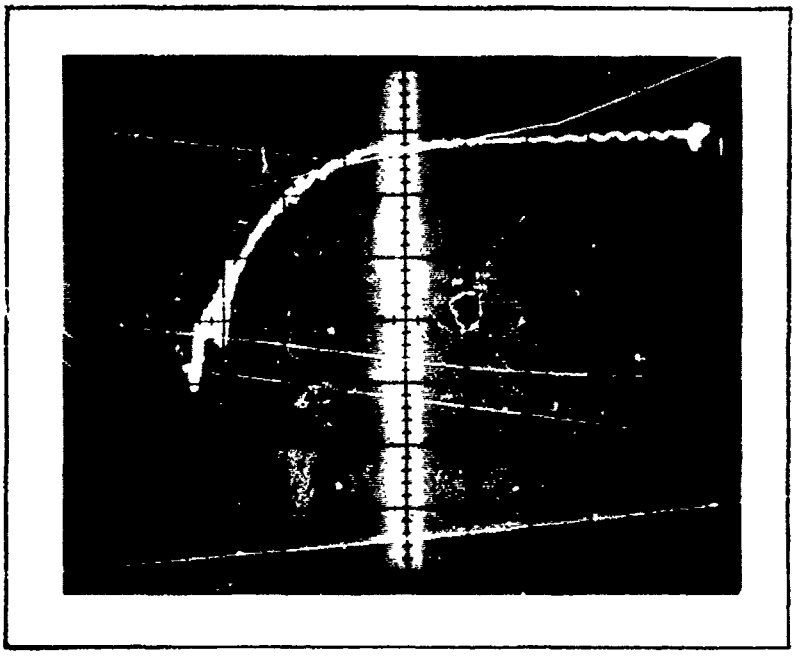

Date: 14 Mar 75

Sample

Snow type: 7 days

T	(°C)	= -34
d	(cm)	= 20.3
h_o	(cm)	= 7.6
A	(cm^2)	= 323.3
V_o	(cm^3)	= 2460
W	(g)	= 742
ρ_o	(gcm^{-3})	= .304
h_f	(cm)	= 3.45
V_f	(cm^3)	= 1113
ρ_f	(gcm^{-3})	= .666

Test No. 26 Rate of deform. ($cm\ sec^{-1}$) = 40

Load: Vert. scale: 1 div. = 2275 (kg)
Stroke: Horiz. scale: 1 div. = 0.51 (cm)

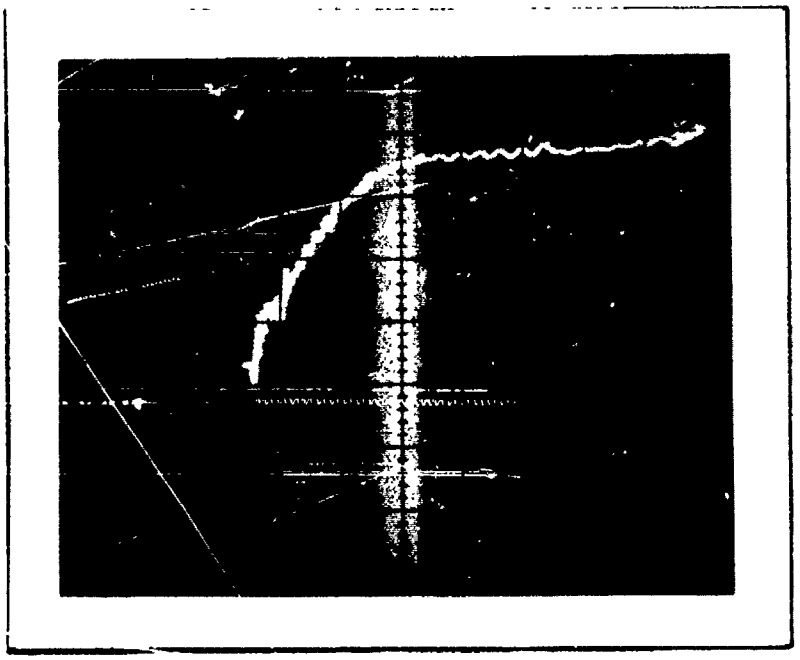

Date: 14 Mar 75

Sample

Snow type: 7 days

T	(°C)	= -34
d	(cm)	= 20.3
h_o	(cm)	= 7.6
A	(cm^2)	= 323.3
V_o	(cm^3)	= 2460
W	(g)	= 863
ρ_o	(gcm^{-3})	= .351
h_f	(cm)	= 4.0
V_f	(cm^3)	= 1291
ρ_f	(gcm^{-3})	= .668

Test No. 27 Rate of deform. ($cm\ sec^{-1}$) = 40

Load: Vert. scale: 1 div. = 2275 (kg)
Stroke: Horiz. scale: 1 div. = 0.51 (cm)

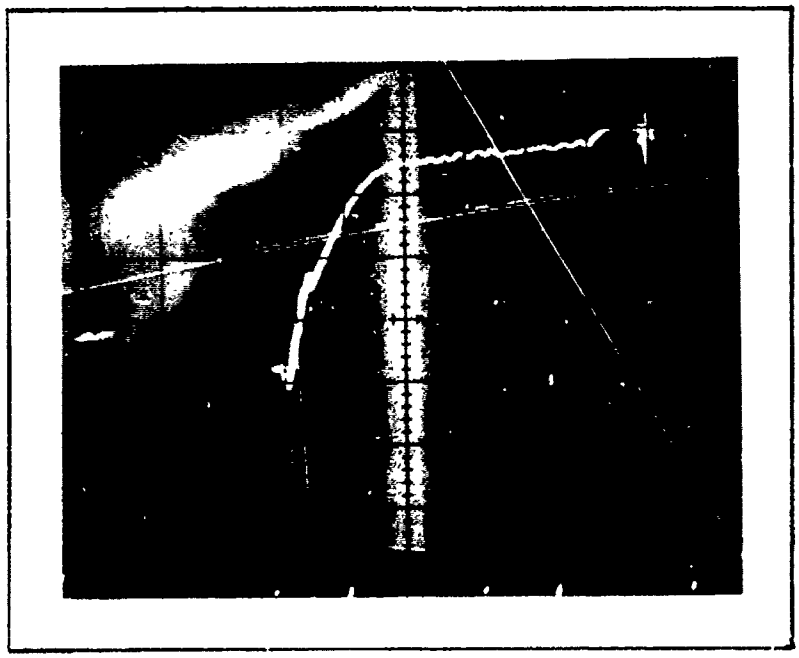

Date: 20 Mar 75

Sample

Snow type: 3 days

T	(°C)	= -4
d	(cm)	= 29.0
h_o	(cm)	= 8.95
A	(cm^2)	= 658
V_o	(cm^3)	= 5880
W	(g)	= 2204
ρ_o	(gcm^{-3})	= .375
h_f	(cm)	= 5.40
V_f	(cm^3)	= 3550
ρ_f	(gcm^{-3})	= .621

Test No. 29 Rate of deform. ($cm\ sec^{-1}$) = 40

Load: Vert. scale: 1 div. = 2275 (kg)
Stroke: Horiz. scale: 1 div. = 0.64 (cm)

CRREL Form 42 (OT)
15 May 74

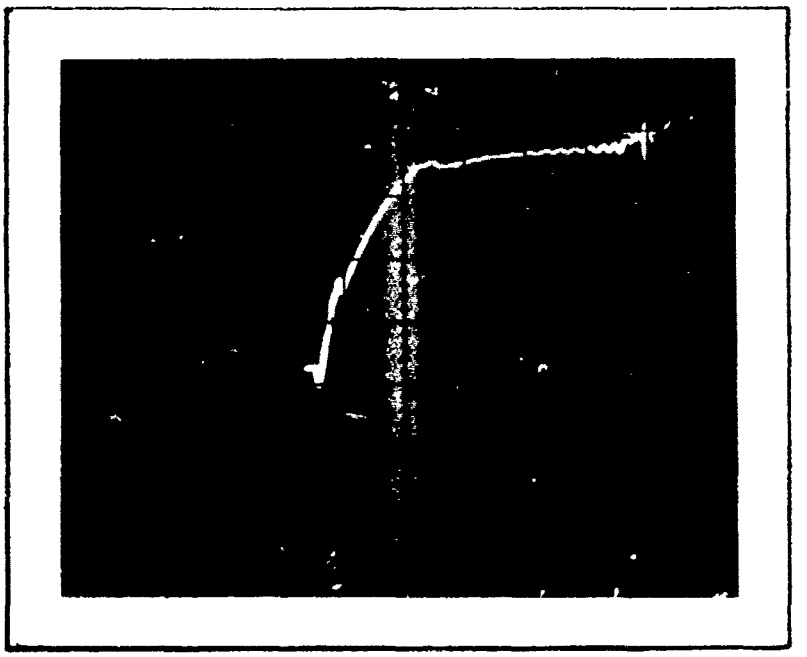

Date: 20 Mar 75

Sample

Snow type: 3 days

T	(°C)	= -4
d	(cm)	= 20.0
h_o	(cm)	= 9.55
A	(cm^2)	= 658
V_o	(cm^3)	= 6280
W	(g)	= 2393
ρ_o	(gcm^{-3})	= .381
h_f	(cm)	= 6.0
V_f	(cm^3)	= 3945
ρ_f	(gcm^{-3})	= .606

Test No. 30 Rate of deform. ($cm\ sec^{-1}$) = 40

Load: Vert. scale: 1 div. = 2275 (kg)
Stroke: Horiz. scale: 1 div. = 0.64 (cm)

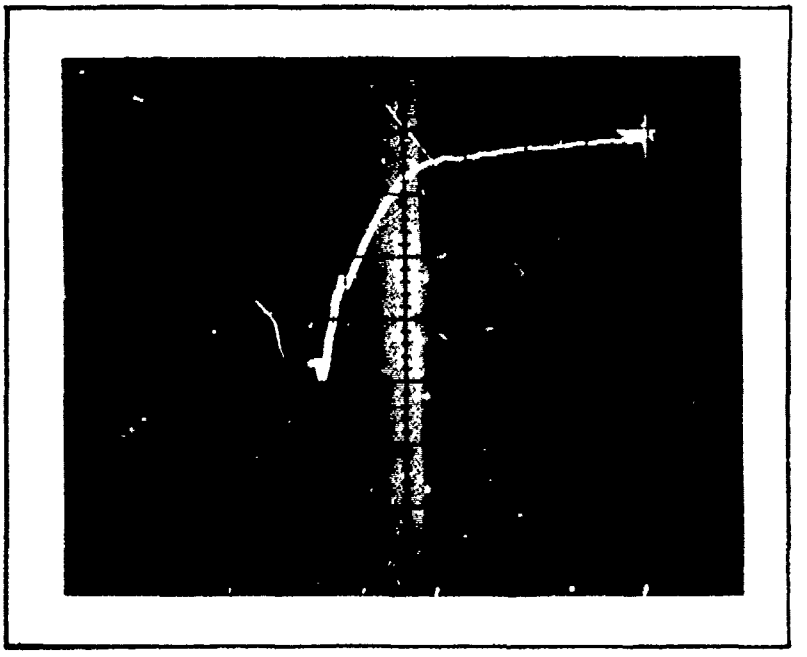

Date: 20 Mar 75

Sample

Snow type: 3 days

T	(°C)	= -4
d	(cm)	= 20.0
h_o	(cm)	= 9.85
A	(cm^2)	= 658
V_o	(cm^3)	= 6475
W	(g)	= 2520
ρ_o	(gcm^{-3})	= .389
h_f	(cm)	= 6.20
V_f	(cm^3)	= 4075
ρ_f	(gcm^{-3})	= .619

Test No. 31 Rate of deform. ($cm\ sec^{-1}$) = 40

Load: Vert. scale: 1 div. = 2275 (kg)
Stroke: Horiz. scale: 1 div. = 0.64 (cm)

CRREL Form 42 (OT)
15 May 74

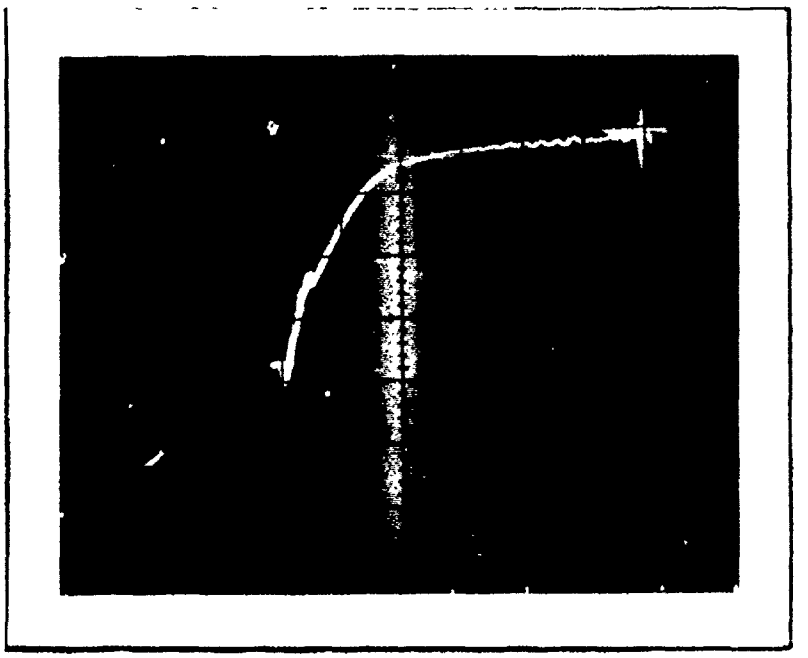

Date: 20 Mar 75

Sample

Snow type: 3 days

T	(^{o}C)	= -4
d	(cm)	= 20.0
h_o	(cm)	= 10.2
A	(cm^2)	= 658
V_o	(cm^3)	= 6675
W	(g)	= 2430
ρ_o	(gcm^{-3})	= .364
h_f	(cm)	= 5.95
V_f	(cm^3)	= 3910
ρ_f	(gcm^{-3})	= .622

Test No. 32 Rate of deform. ($cm\ sec^{-1}$) = 40

Load: Vert. scale: 1 div. = 2275 (kg)
Stroke: Horiz. scale: 1 div. = 0.64 (cm)

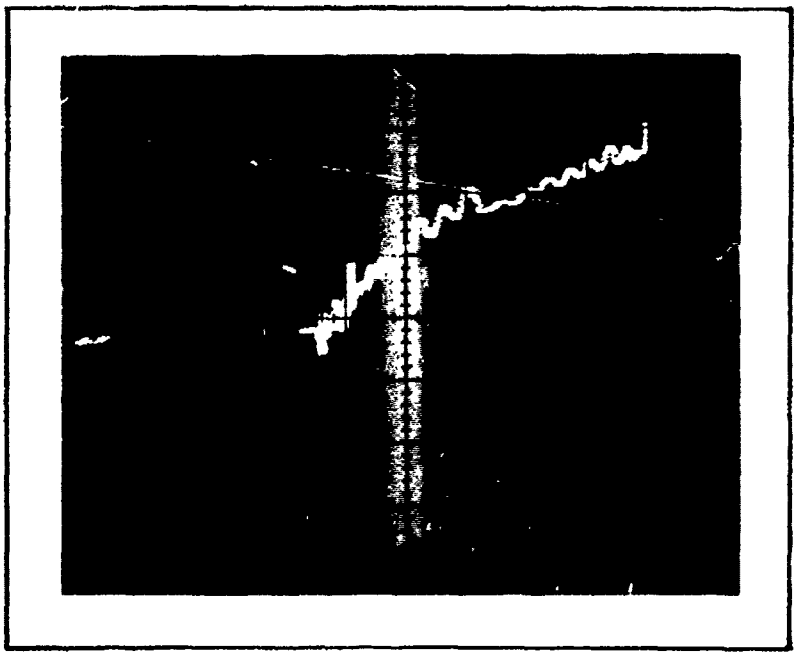

Date: 24 Mar 75

Sample

Snow type: 7 days

T	(^{o}C)	= -10
d	(cm)	= 20.3
h_o	(cm)	= 7.6
A	(cm^2)	= 323.3
V_o	(cm^3)	= 2460
W	(g)	= 1445
ρ_o	(gcm^{-3})	= .588
h_f	(cm)	= 6.0
V_f	(cm^3)	= 1938
ρ_f	(gcm^{-3})	= .746

Test No. 33 Rate of deform. ($cm\ sec^{-1}$) = 40

Load: Vert. scale: 1 div. = 2275 (kg)
Stroke: Horiz. scale: 1 div. = 0.25 (cm)

CRREL Form 42 (OT)
15 May 74

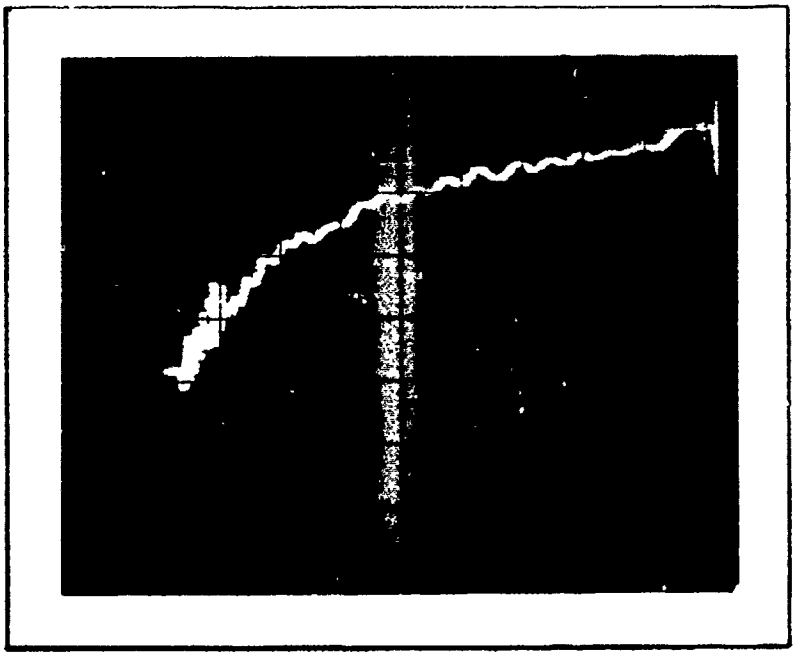

Date: 24 Mar 75

Sample

Snow type: 7 days

T	(^{o}C)	= -34
d	(cm)	= 20.3
h_o	(cm)	= 7.6
A	(cm^2)	= 323.3
V_o	(cm^3)	= 2460
W	(g)	= 1307
ρ_o	(gcm^{-3})	= .531
$h_{\frac{1}{4}}$	(cm)	= 5.60
$V_{\frac{1}{4}}$	(cm^3)	= 1810
$\rho_{\frac{1}{4}}$	(gcm^{-3})	= .722

Test No. 35 Rate of deform. ($cm\ sec^{-1}$) = 40

Load: Vert. scale: 1 div. = 2275 (kg)
Stroke: Horiz. scale: 1 div. = 0.25 (cm)

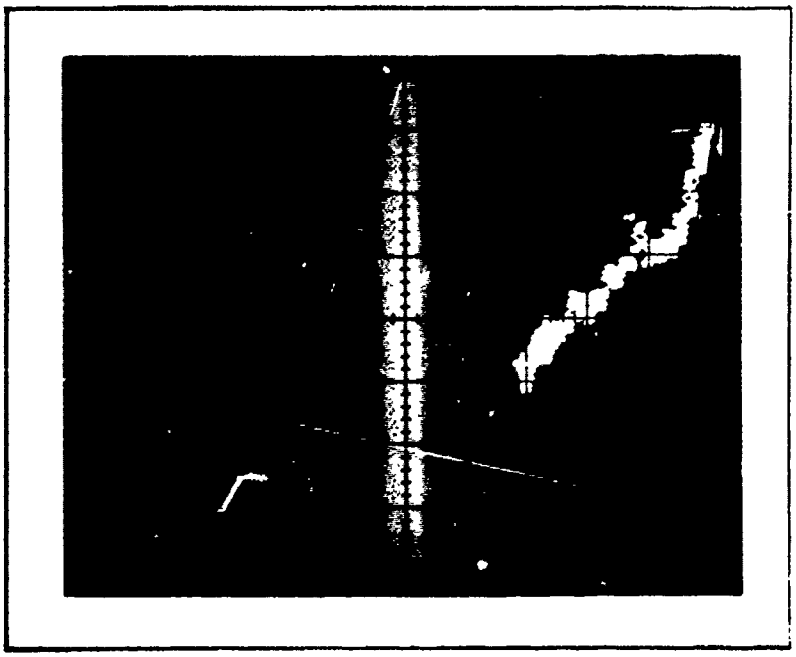

Date: 24 Mar 75

Sample

Snow type: 7 days

T	(^{o}C)	= -34
d	(cm)	= 20.3
h_o	(cm)	= 7.6
A	(cm^2)	= 323.3
V_o	(cm^3)	= 2460
W	(g)	= 1577
ρ_o	(gcm^{-3})	= .641
$h_{\frac{1}{4}}$	(cm)	= 6.90
$V_{\frac{1}{4}}$	(cm^3)	= 2227
$\rho_{\frac{1}{4}}$	(gcm^{-3})	= .708

Test No. 36 Rate of deform. ($cm\ sec^{-1}$) = 40

Load: Vert. scale: 1 div. = 2275 (kg)
Stroke: Horiz. scale: 1 div. = 0.25 (cm)

CRREL Form 42 (OT)
15 May 74

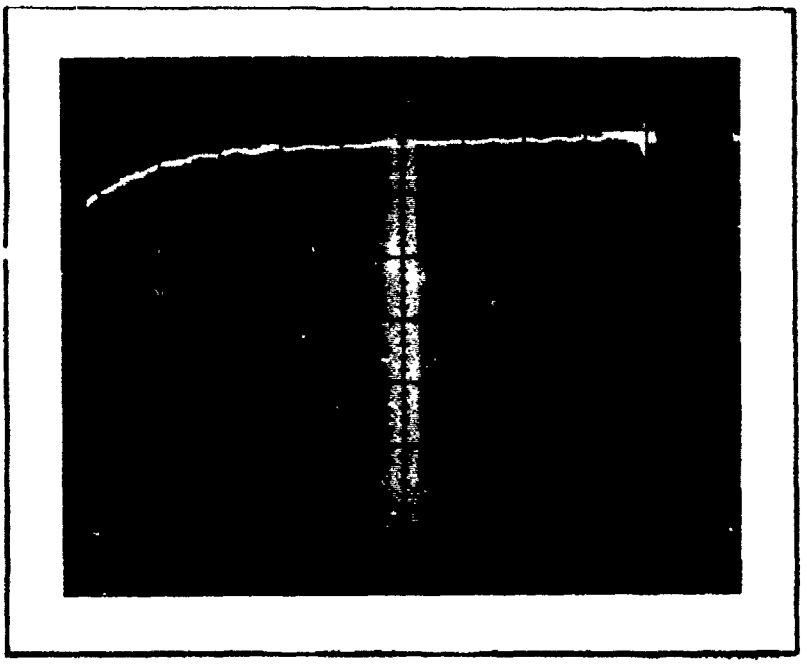

Date: 2 Apr 75

Sample

Snow type: 16 days

T	(°C)	= -34
d	(cm)	= 12.7
h_o	(cm)	= 5.1
A	(cm^2)	= 126.6
V_o	(cm^3)	= 643
W	(g)	= 199
ρ_o	(gcm^{-3})	= .310
h_f	(cm)	= 2.10
V_f	(cm^3)	= 266
ρ_f	(gcm^{-3})	= .749

Test No. 37 Rate of deform. ($cm\ sec^{-1}$) = 40

Load: Vert. scale: 1 div. = 2275 (kg)
Stroke: Horiz. scale: 1 div. = 0.25 (cm)

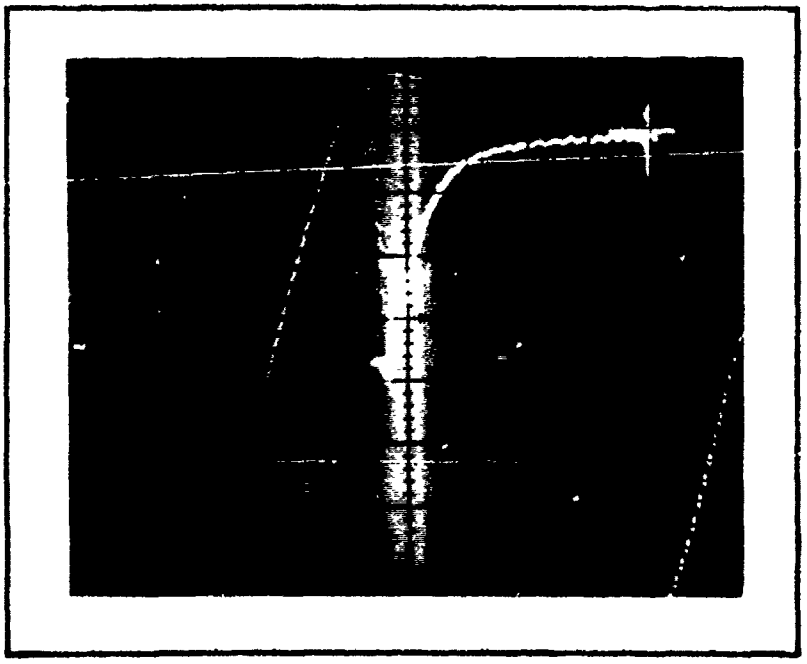

Date: 2 Apr 75

Sample

Snow type: 16 days

T	(°C)	= -34
d	(cm)	= 12.7
h_o	(cm)	= 5.1
A	(cm^2)	= 126.6
V_o	(cm^3)	= 643
W	(g)	= 206
ρ_o	(gcm^{-3})	= .320
h_f	(cm)	= 2.20
V_f	(cm^3)	= 278
ρ_f	(gcm^{-3})	= .741

Test No. 38 Rate of deform. ($cm\ sec^{-1}$) = 40

Load: Vert. scale: 1 div. = 2275 (kg)
Stroke: Horiz. scale: 1 div. = 0.64 (cm)

CRREL Form 42 (OT)
15 May 74

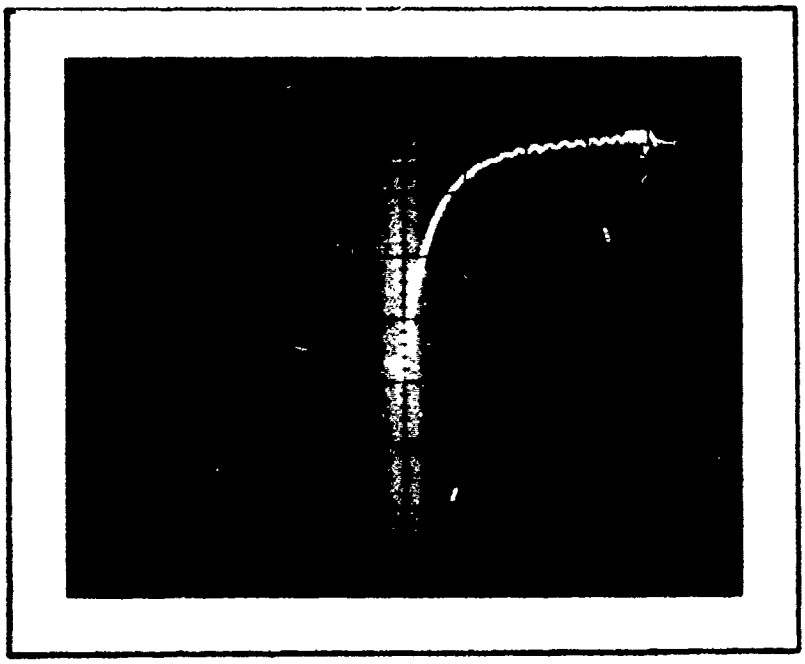

Date: 2 Apr 75

Sample

Snow type: 16 days

T	(°C)	= -34
d	(cm)	= 12.7
h_o	(cm)	= 5.1
A	(cm^2)	= 126.6
V_o	(cm^3)	= 643
W	(g)	= 220
ρ_o	(gcm^{-3})	= .342
$h_{\frac{1}{4}}$	(cm)	= 2.35
$V_{\frac{1}{4}}$	(cm^3)	= 298
$\rho_{\frac{1}{4}}$	(gcm^{-3})	= .740

Test No. 39 Rate of deform. ($cm\ sec^{-1}$) = 40

Load: Vert. scale: 1 div. = 2275 (kg)
Stroke: Horiz. scale: 1 div. = 0.64 (cm)

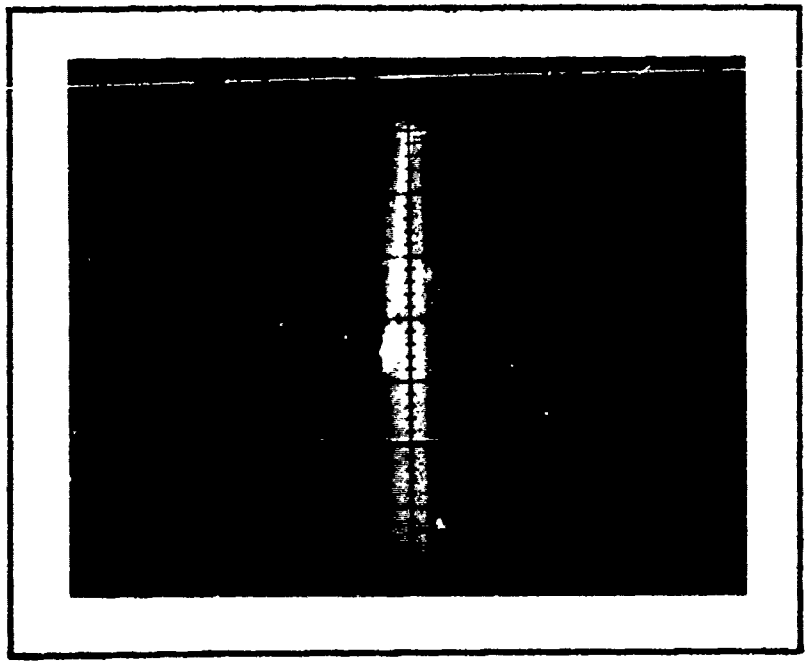

Date: 4 Apr 75

Sample

Snow type: 7 days

T	(°C)	= -34
d	(cm)	= 12.7
h_o	(cm)	= 2.54
A	(cm^2)	= 126.6
V_o	(cm^3)	= 321.5
W	(g)	= 244
ρ_o	(gcm^{-3})	= .760
$h_{\frac{1}{4}}$	(cm)	= 2.46
$V_{\frac{1}{4}}$	(cm^3)	= 311
$\rho_{\frac{1}{4}}$	(gcm^{-3})	= .785

Test No. 40 Rate of deform. ($cm\ sec^{-1}$) = 40

Load: Vert. scale: 1 div. = 2275 (kg)
Stroke: Horiz. scale: 1 div. = 0.25 (cm)

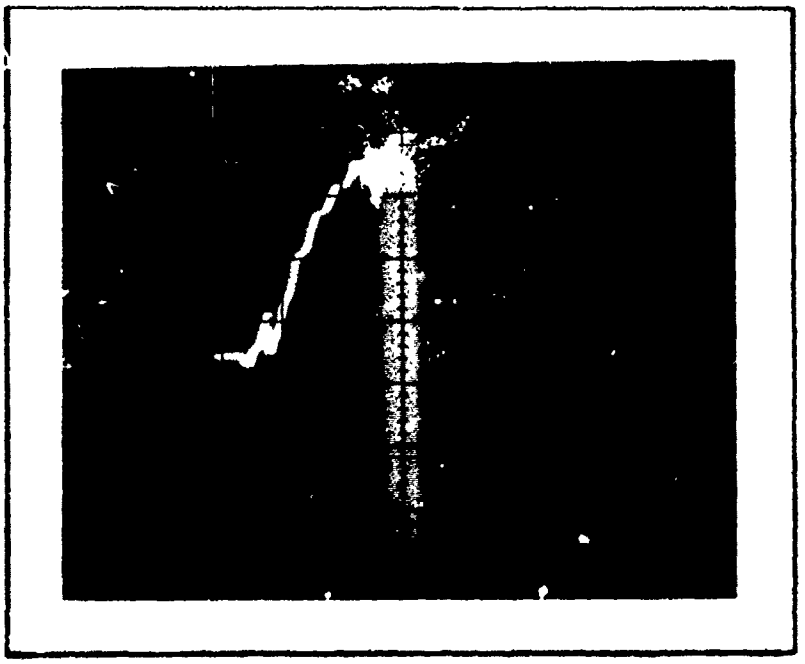

Date: 4 Apr 75

Sample

Snow type: 7 days

T	(^{o}C)	= -1
d	(cm)	= 12.7
h_o	(cm)	= 2.5
A	(cm^2)	= 126.6
V_o	(cm^3)	= 321.5
W	(g)	= 186
ρ_o	(gcm^{-3})	= .580
$h_{\frac{1}{2}}$	(cm)	= 1.68
$V_{\frac{1}{2}}$	(cm^3)	= 212.5
$\rho_{\frac{1}{2}}$	(gcm^{-3})	= .875

Test No. 41 Rate of deform. ($cm\ sec^{-1}$) = 40

Load: Vert. scale: 1 div. = 2275 (kg)
Stroke: Horiz. scale: 1 div. = 0.25 (cm)

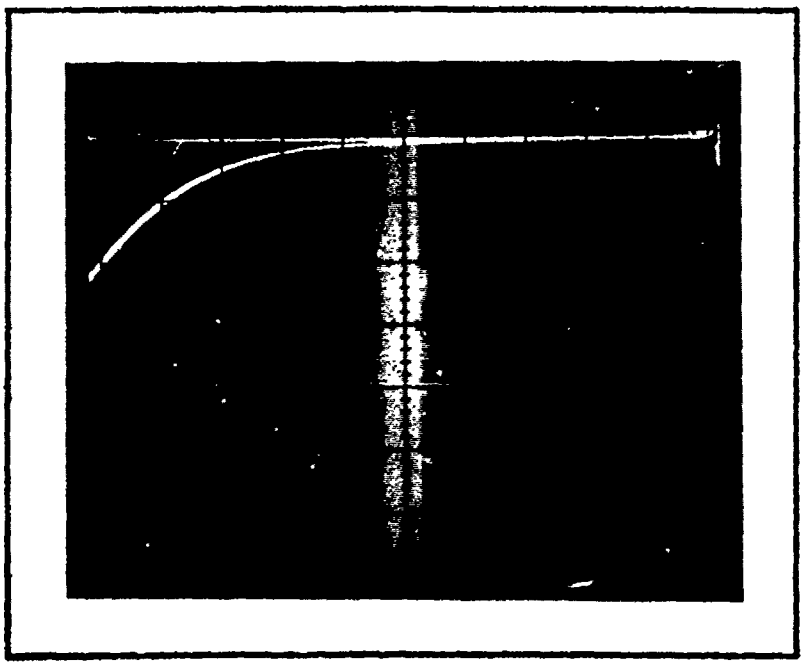

Date: 4 Apr 75

Sample

Snow type: 7 days

T	(^{o}C)	= -1
d	(cm)	= 12.7
h_o	(cm)	= 5.1
A	(cm^2)	= 126.6
V_o	(cm^3)	= 643
W	(g)	= 199
ρ_o	(gcm^{-3})	= .310
$h_{\frac{1}{2}}$	(cm)	= 1.70
$V_{\frac{1}{2}}$	(cm^3)	= 215
$\rho_{\frac{1}{2}}$	(gcm^{-3})	= .91

Test No. 42 Rate of deform. ($cm\ sec^{-1}$) = 40

Load: Vert. scale: 1 div. = 2275 (kg)
Stroke: Horiz. scale: 1 div. = 0.25 (cm)

CRREL Form 42 (OT)
15 May 74

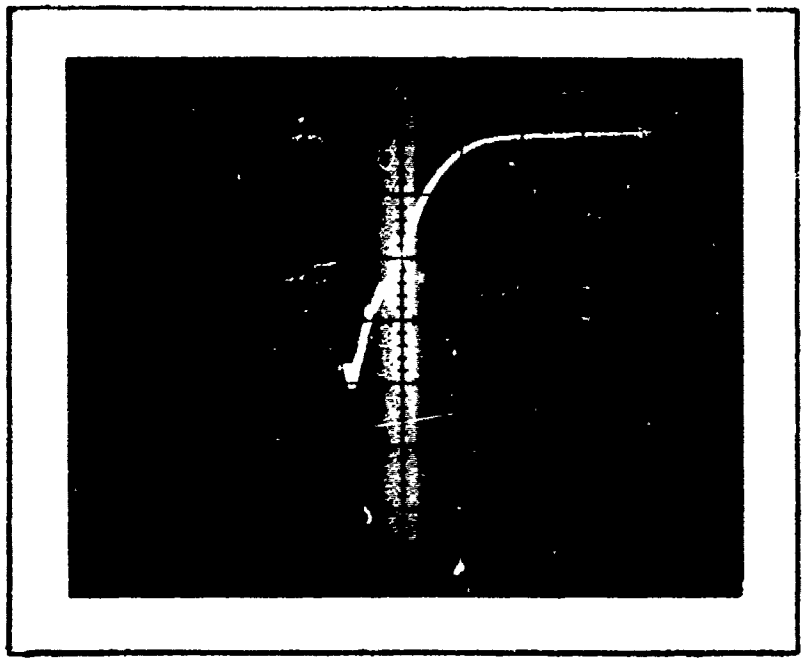

Date: 4 Apr 75

Sample

Snow type: 7 days

T	(^{o}C)	= -1
d	(cm)	= 12.7
h_o	(cm)	= 5.1
A	(cm^2)	= 126.6
V_o	(cm^3)	= 643
W	(g)	= 201
ρ_o	(gcm^{-3})	= .313
h_f	(cm)	= 1.70
V_f	(cm^3)	= 215
ρ_f	(gcm^{-3})	= .91

Test No. 43 Rate of deform. ($cm\ sec^{-1}$) = 40

Load: Vert. scale: 1 div. = 2275 (kg)
Stroke: Horiz. scale: 1 div. = 0.64 (cm)

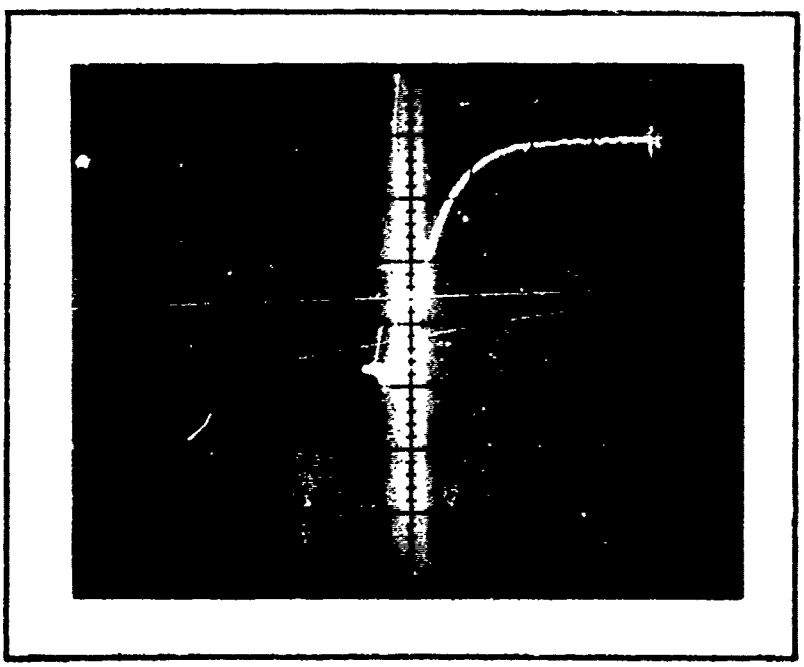

Date: 4 Apr 75

Sample

Snow type: 7 days

T	(^{o}C)	= -1
d	(cm)	= 20.3
h_o	(cm)	= 5.1
A	(cm^2)	= 323.3
V_o	(cm^3)	= 1633
W	(g)	= 492
ρ_o	(gcm^{-3})	= .301
h_f	(cm)	= 1.90
V_f	(cm^3)	= 614
ρ_f	(gcm^{-3})	= .801

Test No. 44 Rate of deform. ($cm\ sec^{-1}$) = 40

Load: Vert. scale: 1 div. = 2275 (kg)
Stroke: Horiz. scale: 1 div. = 0.64 (cm)

CRREL Form 42 (OT)
15 May 74

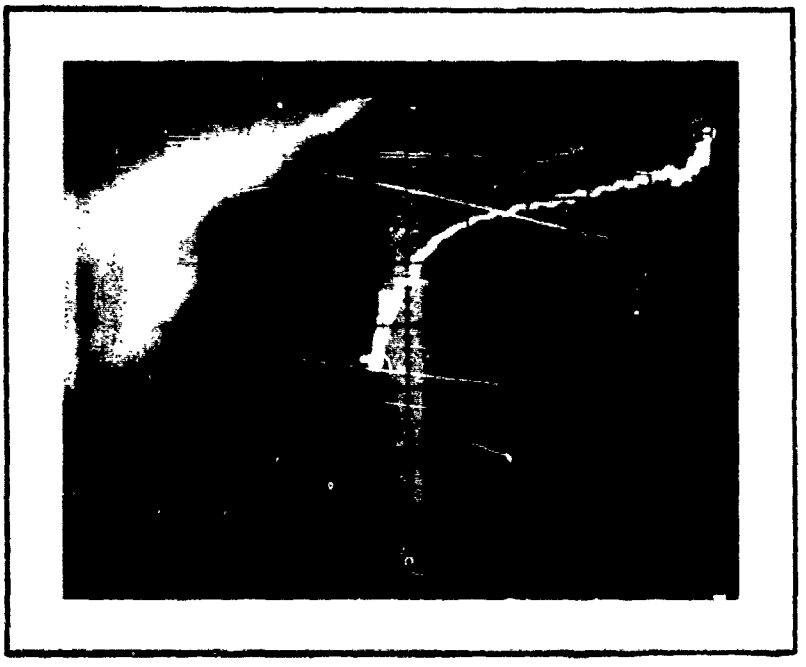

Date: 10 Apr 75

Sample

Snow type: 3 days

T	(°C)	= -34
d	(cm)	= 20.3
h_o	(cm)	= 5.1
A	(cm^2)	= 323.3
V_o	(cm^3)	= 1633
W	(g)	= 817
ρ_o	(gcm^{-3})	= .500
h_f	(cm)	= 3.65
V_f	(cm^3)	= 1179
ρ_f	(gcm^{-3})	= .694

Test No. 45 Rate of deform. ($cm\ sec^{-1}$) = 40

Load: Vert. scale: 1 div. = 2275 (kg)
Stroke: Horiz. scale: 1 div. = 0.25 (cm)

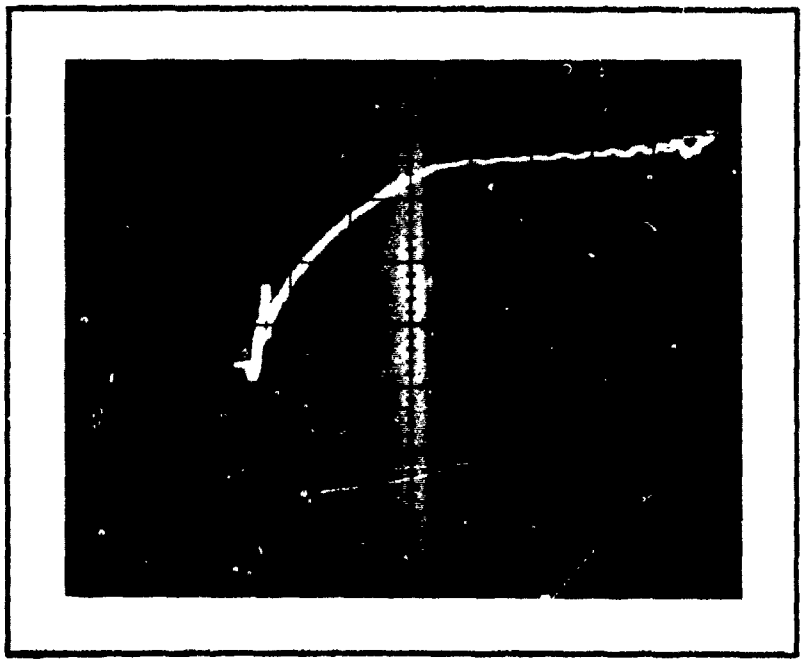

Date: 10 Apr 75

Sample

Snow type: 3 days

T	(°C)	= -34
d	(cm)	= 12.7
h_o	(cm)	= 5.1
A	(cm^2)	= 126.6
V_o	(cm^3)	= 643
W	(g)	= 290
ρ_o	(gcm^{-3})	= .451
h_f	(cm)	= 3.0
V_f	(cm^3)	= 380
ρ_f	(gcm^{-3})	= .764

Test No. 46 Rate of deform. ($cm\ sec^{-1}$) = 40

Load: Vert. scale: 1 div. = 2275 (kg)
Stroke: Horiz. scale: 1 div. = 0.25 (cm)

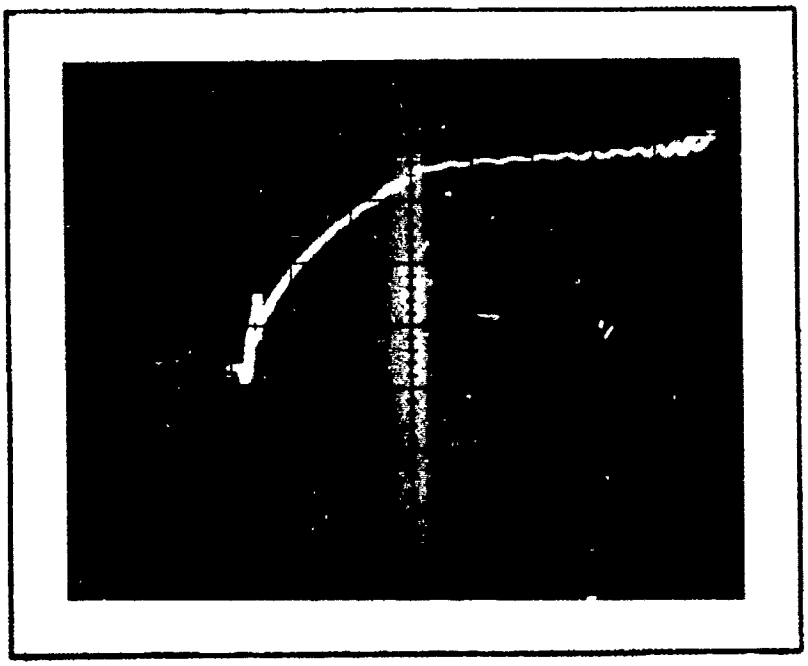

Date: 10 Apr 75

Sample

Snow type: 3 days

T	(°C)	= -34
d	(cm)	= 12.7
h_o	(cm)	= 5.1
A	(cm^2)	= 126.6
V_o	(cm^3)	= 643
W	(g)	= 287
ρ_o	(gcm^{-3})	= .447
$h_{\frac{1}{2}}$	(cm)	= 3.0
$V_{\frac{1}{2}}$	(cm^3)	= 380
$\rho_{\frac{1}{2}}$	(gcm^{-3})	= .756

Test No. 47 Rate of deform. ($cm\ sec^{-1}$) = 40

Load: Vert. scale: 1 div. = 2275 (kg)
Stroke: Horiz. scale: 1 div. = 0.25 (cm)

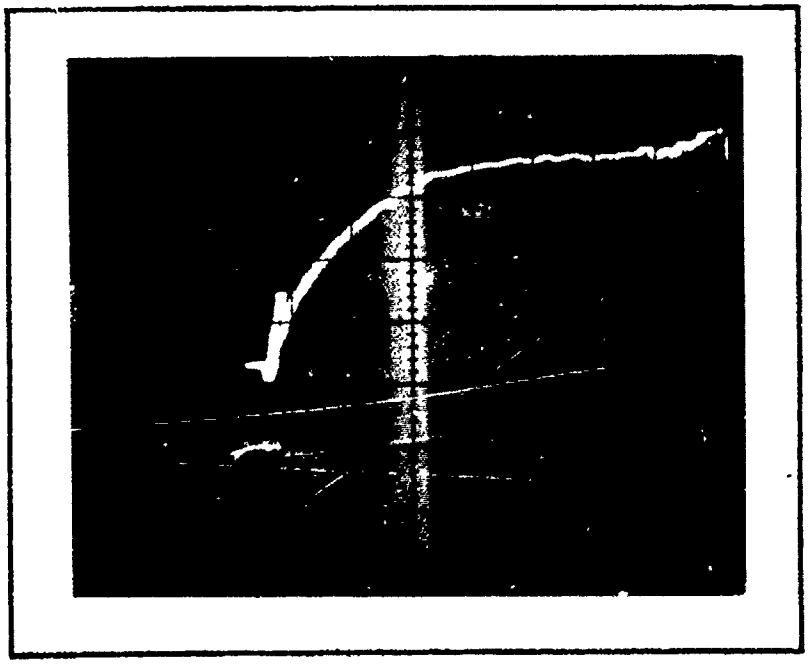

Date: 10 Apr 75

Sample

Snow type: 3 days

T	(°C)	= -34
d	(cm)	= 12.7
h_o	(cm)	= 5.1
A	(cm^2)	= 126.6
V_o	(cm^3)	= 643
W	(g)	= 311
ρ_o	(gcm^{-3})	= .484
$h_{\frac{1}{2}}$	(cm)	= 3.20
$V_{\frac{1}{2}}$	(cm^3)	= 405
$\rho_{\frac{1}{2}}$	(gcm^{-3})	= .769

Test No. 48 Rate of deform. ($cm\ sec^{-1}$) = 40

Load: Vert. scale: 1 div. = 2275 (kg)
Stroke: Horiz. scale: 1 div. = 0.25 (cm)

CRREL Form 42 (OT)
15 May 74

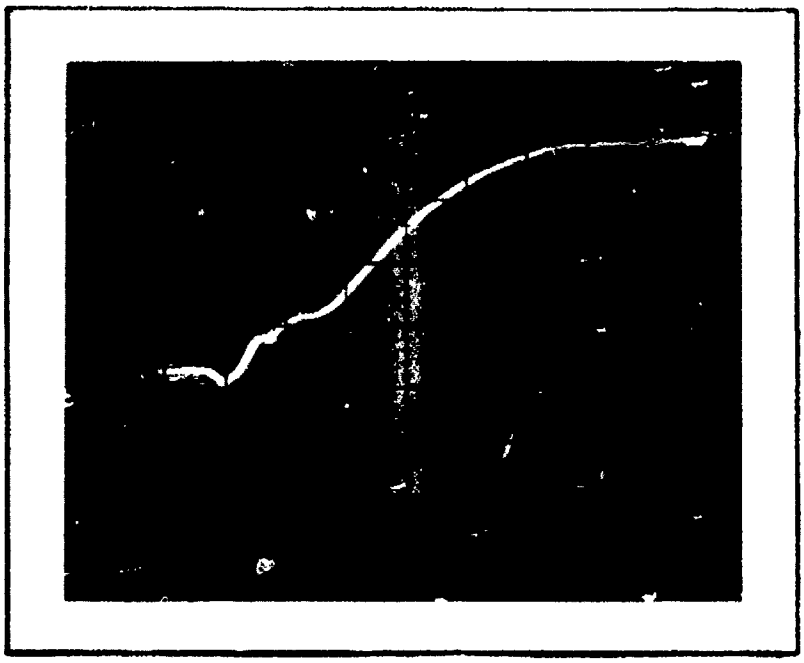

Date: 10 Apr 75

Sample

Snow type: 3 days

T	(^{o}C)	= -1
d	(cm)	= 12.7
h_o	(cm)	= 5.1
A	(cm^2)	= 126.6
V_o	(cm^3)	= 643
W	(g)	= 297
ρ_o	(gcm^{-3})	= .462
h_1	(cm)	= 2.65
V_1	(cm^3)	= 335
ρ_1	(gcm^{-3})	= .888

Test No. 40 Rate of deform. ($cm\ sec^{-1}$) = 40

Load: Vert. scale: 1 div. = 2275 (kg)
Stroke: Horiz. scale: 1 div. = 0.25 (cm)

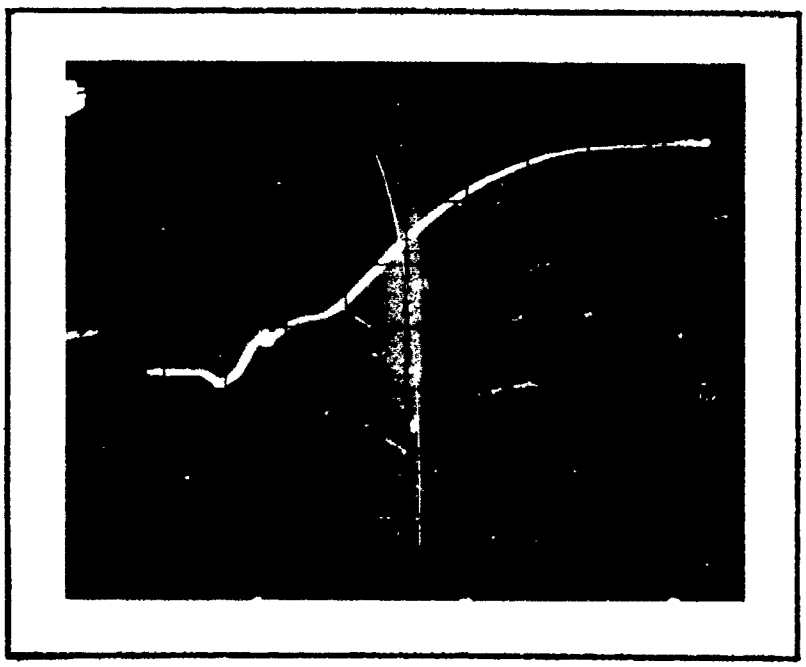

Date: 10 Apr 75

Sample

Snow type: 3 days

T	(^{o}C)	= -1
d	(cm)	= 12.7
h_o	(cm)	= 5.1
A	(cm^2)	= 126.6
V_o	(cm^3)	= 643
W	(g)	= 301
ρ_o	(gcm^{-3})	= .468
h_1	(cm)	= 2.60
V_1	(cm^3)	= 329
ρ_1	(gcm^{-3})	= .91

Test No. 50 Rate of deform. ($cm\ sec^{-1}$) = 40

Load: Vert. scale: 1 div. = 2275 (kg)
Stroke: Horiz. scale: 1 div. = 0.25 (cm)

CRREL Form 42 (OT)
15 May 74

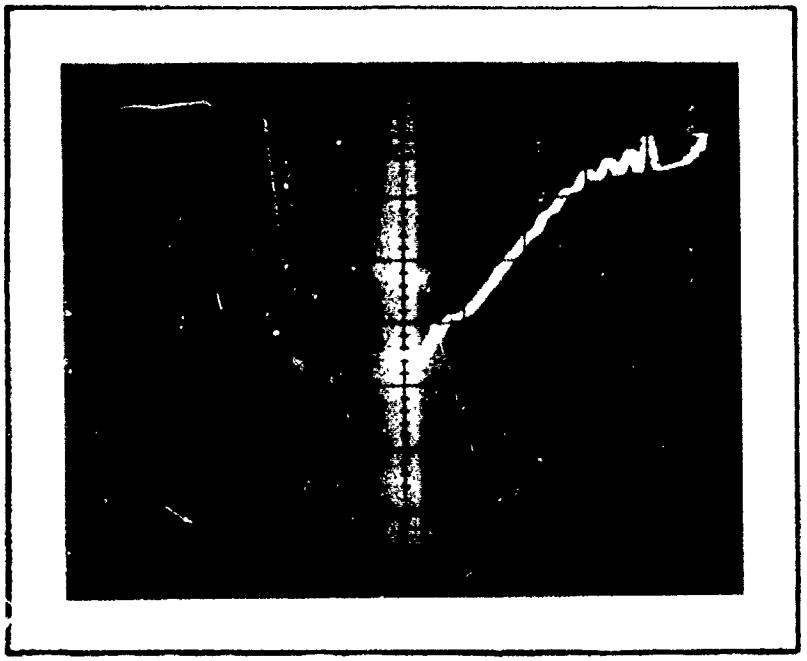

Date: 10 Apr 75

Sample

Snow type: 3 days

T	(^{o}C)	= -1
d	(cm)	= 20.3
h_o	(cm)	= 5.1
A	(cm^2)	= 323.3
V_o	(cm^3)	= 1633
W	(g)	= 847
ρ_o	(gcm^{-3})	= .518
$h_{\frac{1}{3}}$	(cm)	= 3.65
$V_{\frac{1}{3}}$	(cm^3)	= 1179
$\rho_{\frac{1}{3}}$	(gcm^{-3})	= .719

Test No. 51 Rate of deform. ($cm\ sec^{-1}$) = 40

Load: Vert. scale: 1 div. = 2275 (kg)
Stroke: Horiz. scale: 1 div. = 0.25 (cm)

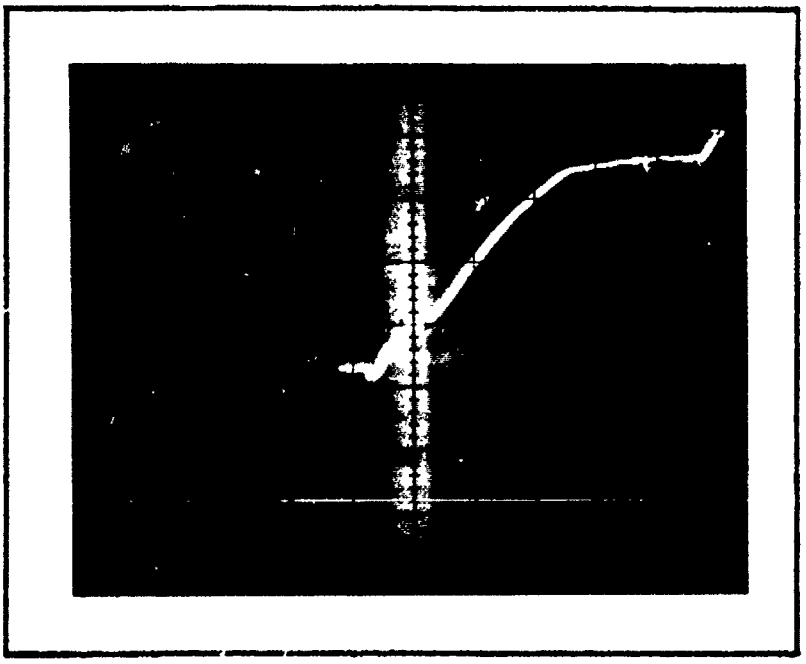

Date: 10 Apr 75

Sample

Snow type: 3 days

T	(^{o}C)	= -1
d	(cm)	= 20.3
h_o	(cm)	= 5.1
A	(cm^2)	= 323.3
V_o	(cm^3)	= 1633
W	(g)	= 807
ρ_o	(gcm^{-3})	= .494
$h_{\frac{1}{3}}$	(cm)	= 3.50
$V_{\frac{1}{3}}$	(cm^3)	= 1130
$\rho_{\frac{1}{3}}$	(gcm^{-3})	= .714

Test No. 52 Rate of deform. ($cm\ sec^{-1}$) = 40

Load: Vert. scale: 1 div. = 2275 (kg)
Stroke: Horiz. scale: 1 div. = 0.25 (cm)

CRREL Form 42 (OT)
15 May 74